

UCLA

UCLA Previously Published Works

Title

A Simple Estimation Method of Weibull Modulus and Verification with Strength Data

Permalink

<https://escholarship.org/uc/item/08j1x13w>

Journal

Applied Sciences, 9(8)

ISSN

2076-3417

Author

Ono, Kanji

Publication Date

2019


DOI

10.3390/app9081575

Peer reviewed

Review

A Simple Estimation Method of Weibull Modulus and Verification with Strength Data

Kanji Ono 

Department of Materials Science and Engineering, University of California, Los Angeles (UCLA), Los Angeles, CA 90095, USA; ono@ucla.edu; Tel.: 1-310-825-5534

Received: 17 March 2019; Accepted: 12 April 2019; Published: 16 April 2019



Abstract: This study examines methods for simplifying estimation of the Weibull modulus. This parameter is an important instrument in understanding the statistical behavior of the strength of materials, especially those of brittle solids. It is shown that a modification of Robinson's approximate expression can provide good estimates of Weibull modulus values (m) in terms of average strength ($\langle\sigma\rangle$) and standard deviation (S): $m = 1.10 \langle\sigma\rangle/S$. This modified Robinson relation is verified on the basis of 267 Weibull analyses accompanied by $\langle\sigma\rangle$ and S measurements. Estimated m values matched normally obtained m values on average within 1%, and each pair of m values was within $\pm 20\%$, except for 11 cases. Applications are discussed, indicating that the above relation can offer a quantitative tool based on the Weibull theory to engineering practice. This survey suggests a rule of thumb: wrought metal alloys have Weibull moduli of 10 to 200.

Keywords: Weibull modulus; estimation methods; modified Robinson relation; strength data; observed datasets; large-scale data

1. Introduction

Weibull first used a statistical distribution in 1939 [1] that is now known as the Weibull distribution to characterize the fracture strength of nine different materials, totaling 20 different types of samples with several loading modes. These included 2000 to 3000 cotton fiber and yarn samples, while 20 to 128 samples were typically tested for metals, with the total sample counts nearing 8000. He extended its applications to broader categories in 1951 [2]. The Weibull distribution has since been applied in wide-ranging fields in engineering and beyond [3]. While the present work is directed to the analysis of material strength, mainly from tensile and flexure testing, the lifetime prediction of engineering structures and various systems and components is another branch of statistical analysis where the Weibull distribution plays a key role [4,5]. Several recent examples of such applications can be found in [6–10]. It is an important tool for enhancing the precision of measurements that tend to show wide deviation.

Two-parameter Weibull distribution, the most basic form, describes the probability of failure P by [1–3]:

$$1 - P = \exp\{-(\sigma/\sigma_0)^m\}, \quad (1)$$

where m is the Weibull modulus (also called the shape parameter), σ_0 is the scale parameter, and σ is the variable (fracture strength in this study), respectively. The basis of this distribution is given in terms of the weakest link theory; see Robinson and Batdorf [11,12]. From N fracture tests, a cumulative probability distribution curve is obtained as a function of (σ/σ_0) . In a graphical approach, one can follow Weibull [1], plotting $\ln(-\ln(1 - P))$ against $\ln(\sigma)$ or $\ln(\sigma/\sigma_0)$, and obtaining a best fit line, the slope of which equals m . The scale parameter, σ_0 , is slightly larger than the average fracture strength $\langle\sigma\rangle$, and these are related by [3,13,14]:

$$\langle \sigma \rangle = \sigma_0 \Gamma(1 + 1/m), \quad (2)$$

where $\Gamma(x)$ is the gamma function. This Equation (2) can be approximated by [15]:

$$\langle \sigma \rangle = \sigma_0 (1 + 0.276 m^{-0.776}). \quad (3)$$

Numerous methods and software have become available, and the above procedure mainly serves as a learning tool. Still, for untrained users, the initial hurdle for conducting Weibull analysis can hardly be trivial. A survey of online Weibull calculators reveals a confusing and intimidating array of approaches. Regardless of the method used, reliable Weibull parameters can only be obtained from at least $N = 10$ to 20 , since Robinson showed that the coefficient of variation (CV) for m is equal to $1/\sqrt{N}$ [11]. Ritter et al. [16] also arrived at this equation. For $N = 10$, $CV = 0.32$, and this is reduced only to 0.22 , even for $N = 20$. For materials that have higher m values such as fiber-reinforced composites, the N value is specified in technical standards as five or more ($N \geq 5$) [17–19]. However, at $N = 5$, $CV = 0.45$; that is, a large deviation in m needs to be anticipated. See also recent studies on this subject [20,21]. Note that in these statistical works, N is referred to as sample size instead of sample count, which is used here to differentiate the concept from physical dimensions.

Another need for Weibull modulus values is to use them as quality indicators. In ceramics fields, it has been common to indicate the brittleness of materials, since the m values of most ceramics (and cast iron, another brittle material) are 10 or lower. This is in contrast to typical metal alloys, which are generally believed to show $m > 100$ [22], but with a limited number of published reports of high m values. A research project on bridge maintenance [23] identified a Weibull modulus of >70 for undamaged suspension bridge cable wires, whereas an m value of 10 represents cracked, highly corroded wires with two more stages of corrosion between them. Meanwhile, an m value of ~ 30 indicates Stage 4 corrosion, and an m value of ~ 50 indicates Stage 3 corrosion. For this purpose, even approximate m values allow bridge inspectors to classify wires between different corrosion stages quantitatively instead of relying on visual observation. When only limited data is available, with N values less than 10 , efforts of Weibull analysis may be unrewarding, and simpler approximate methods are adequate. In other cases, only average values and their standard deviation (or variance) are available, e.g., from engineering reports or from historical documents.

Simple methods for estimating m values have been discussed in the literature, and these will be examined. Strength data compiled in two interlaboratory studies [24,25] was analyzed to provide Weibull modulus values for five common metal alloys in Section 3, followed by a comparison with a database of Weibull analyses on the fracture or tensile strength of many solids. The simplest, one-parameter method will be verified to best represent more than 260 datasets. Discussion and summary conclude this study.

2. Approximate Methods of Weibull Modulus Estimation

The most common index of data scatter assumes the normal (or Gaussian) distribution and determines the average $\langle \sigma \rangle$ and its standard deviation, S . Another is the Weibull distribution, as shown in Equation (1). These parameters are related. Equation (2) above connects the $\langle \sigma \rangle$ value to the Weibull parameters, σ_0 and m . Similarly, standard deviation, S , is given by [3,11,13,14]:

$$S = \sigma_0 [\Gamma(1 + 2/m) - (\Gamma(1 + 1/m))^2]^{0.5}, \quad (4)$$

where $\Gamma(x)$ is again the gamma function. See [14] for the steps of its derivation. Note that $\Gamma(x)$ is readily available in Microsoft Excel[®] (version 16.16.8, Microsoft, Redmond, WA, USA, 2016). When Equations (2) and (4) are combined, the coefficient of variation, CV, is defined as [3,11,13,14]:

$$CV = S/\langle \sigma \rangle = [\Gamma(1 + 2/m) - (\Gamma(1 + 1/m))^2]^{0.5}/\Gamma(1 + 1/m). \quad (5)$$

CV is a function only of m , and is bounded by $1/m$ and $(\pi/\sqrt{6})/m = 1.283/m$ [13]. In expressing m in terms of the inverse of CV, we have two bounds:

$$m = 1/CV = \langle\sigma\rangle/S \quad \text{and} \quad m = 1.283/CV = 1.283\langle\sigma\rangle/S. \tag{6}$$

This implies that m can be approximated by $\langle\sigma\rangle/S$ or the inverse of CV. In 1972, Robinson [11] first derived this relationship between m and $\langle\sigma\rangle/S$ (or $1/CV$), and also gave approximate expressions as:

$$m = 1.2 \langle\sigma\rangle/S, \tag{7}$$

and:

$$m = (\langle\sigma\rangle/S)^{1.064}, (1.1 < m < 60). \tag{8}$$

Equation (7), or the Robinson relation, has 15% error at $m = 2$, going down to a 6% error at $m = 100$. Equation (8) has 1% error for $1.1 < m < 60$. When two constants are used, Equation (5) can be represented as:

$$m = 1.0461 \cdot (\langle\sigma\rangle/S)^{1.049}, (R^2 = 0.9997), \tag{9}$$

achieving an excellent match. In practice, this can be deemed exact. When numerical values are calculated for CV using Equation (5) by supplying a series of m values, one can then exchange the two sequences, making CV a variable. Thus, Equations (7), (8), and (9) can be compared to Equation (5) and it is found that the last two indeed represent the values of m well. In contrast, Equation (7) has about 7% error. A regression analysis of CV versus m from Equation (5) (with an m value of 1.1 to 127) produces a linear equation with a constant of 1.271 in lieu of 1.2 in Equation (7), yielding a high regression coefficient of $R^2 = 0.9999$. This is a slight improvement over Equation (9). Thus, Robinson's Equation (7) can be converted to an essentially exact representation using:

$$m = 1.271 \langle\sigma\rangle/S. \tag{10}$$

In 1981, Ritter et al. [16] derived Robinson Equation (7) as an approximation for $m > 2$. However, their method is questionable, since the actual constant (\sqrt{K}) from their equation (A29) varies from 1.05 at $m = 2$ to 1.25 at $m = 20$, reaching the upper limit of 1.283 at $m = 60$. They selected the constant to be $\sqrt{1.44} = 1.20$, which is only valid at $m = 9 \pm 1$. Thus, their value appears to be an arbitrary choice, which happened to coincide with Robinson's constant. The Ritter equation was incorporated into ASTM C1499 [26]. By 1986, it was apparently well-known, as Wetherhold [27] used it to confirm the m values he obtained using the corresponding CV values. In 1989, van der Zweig [28] presented the same Robinson relation, but without citing prior works [11,16,26]. Three more approximate expressions have been published by [29–31] as follows (in the order of appearance):

$$m = 1.277 \langle\sigma\rangle/S - 0.462, (5 < m < 50), \tag{11}$$

$$m = 1.272 \langle\sigma\rangle/S - 0.525, \tag{12}$$

$$m = 1.177 \langle\sigma\rangle/S - 0.407, \tag{13}$$

(for $N = 20$).

Equations (11) and (12) were obtained using Monte Carlo simulation as the basis. All five approximations satisfy the bounds for m , except at $m < 1.67$ to 2.3 for Equations (11)–(13). These six approximations are close to the essentially exact Equation (10). When a systematic error of up to 10% to 20% is acceptable, any one of them can be used. However, the merit of using them has vanished, since the linear Equation (10) with $R^2 = 0.9999$ can easily be used. Furthermore, in Section 4, it will be shown that experimentally obtained m values can be represented well using the Robinson relation (Equation (7)) with a reduced constant of 1.1, or $m = 1.1 \langle\sigma\rangle/S$.

In conducting the Weibull analysis of real data, N is limited, and the m value contains an error that depends on N and m [11,16,20,21]. Thus, it is necessary to search for one equation that can best match all the observed m values and is convenient to use. Clearly, the one-parameter expressions of Equations (8) and (10) are preferable and will be considered in the next section. Numerical constants will be varied to achieve a match with the observed m values using a large database of Weibull analyses of material strength from the literature.

3. Weibull Moduli of Five Metal Alloys

ASTM Committee E28 on Mechanical Testing conducted an interlaboratory study on automated ball indentation testing, which included controlled tests of the tensile strength of four alloys, Al 6061-T651, Al 7075-T651, steel 1018, and steel 4142 [24]. The tensile strength datasets of 30 samples each were analyzed for this study to determine the Weibull modulus values for these common metal alloys. The bias of individual laboratory results was corrected based on the average deviation with global average for four alloys. The method discussed in Section 1 was used to obtain the m_{obs} values from the Weibull plots. The scale parameter, σ_0 , was obtained using Equation (2). Weibull plots for the four alloys are shown in Figure 1, and m_{obs} values of 124.0, 91.4, 73.8, and 78.1 were obtained as noted in the figure. Separately, the corresponding m_{est} values were estimated from the values of $\langle\sigma\rangle$ and S using $m = 1.1\langle\sigma\rangle/S$, yielding 124.9, 91.9, 73.3, and 77.8. The two sets matched well within $\pm 1\%$. Another interlaboratory study under strict test protocol was conducted in Europe [25]. It produced a special ingot, from which 200 bars of Nimonic[®] 75 Ni-base alloy (Special Metals Corp, Huntington, WV, USA) were fabricated. The tensile strength data from 18 bars of this Nimonic[®] 75 alloy [25] was analyzed for the Weibull modulus, and $m = 125.3$ was obtained, as shown in Figure 1. The corresponding m_{est} value was 129.7, matching to $+3\%$. Thus, the commonly cited value for wrought metal alloys ($m > 100$) is reasonable for these Al and Ni alloys, but appears $\sim 25\%$ too high for ductile steels. More than 20 m values above 50 are included in the metals data below, but some, including pure copper, were below an m value of 20. More comprehensive testing is needed to better define the ranges of m values for various material types beyond those surveyed in this work.

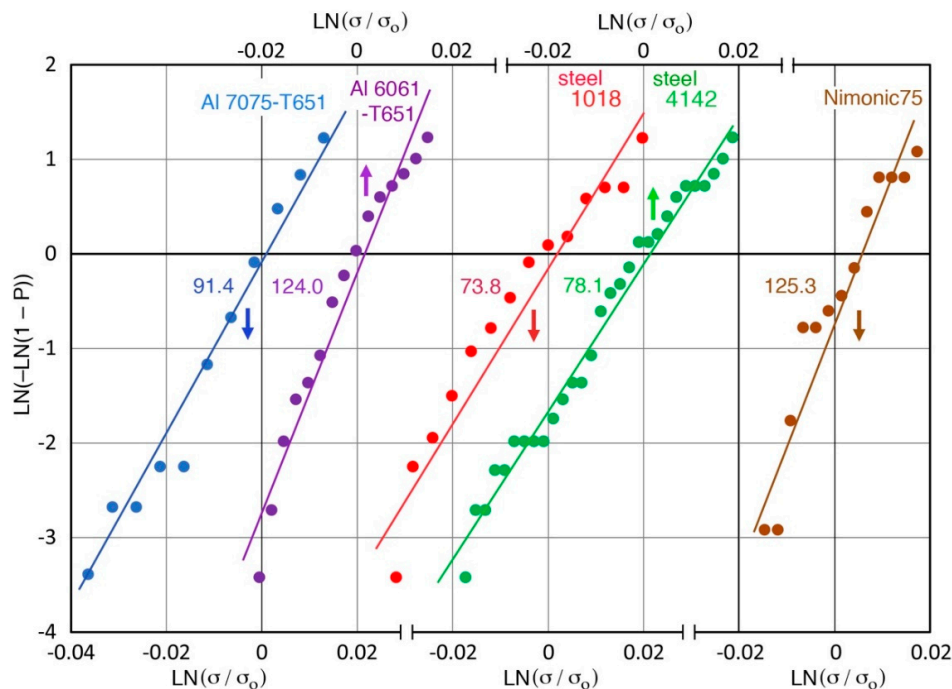


Figure 1. Weibull plots of the tensile strength of five structural alloys: Al 7075-T651 (in blue symbols), Al 6061-T651 (in purple), steel 1018 (in red), steel 4142 (in green), and Nimonic[®] 75 Ni alloy (in brown). Data from [24,25]. Values of m are shown. The horizontal axis is shifted to avoid overlaps.

4. Material Strength Data

The availability of Weibull modulus values is limited in comparison to the more commonly reported values of the average and standard deviation of the tensile (or yield) strength. Most of the data that is collected is from tensile testing for metals, fibers, and composites, whereas flexure testing is more common in ceramics and glasses. Limited fracture data is also included. Fracture toughness data that is suitable for this study is even more difficult to find. Even in the large-scale round-robin study of fracture toughness reported by Wallin [32], K_{Jc} (K_{Ic} by J-integral estimation) values were only given in graphical form without the average and standard deviation. However, their data clearly showed two distinct regimes for ductile and brittle fracture, implying high and low m values. This data style is understandable, as their main aim was to establish the master curve for describing the ductile–brittle transition behavior. The master curve approach is now established as ASTM E1921 standard test method [33], which incorporated a three-parameter Weibull distribution to describe the ductile–brittle transition behavior (test temperature dependence of K_{Jc}). A Weibull modulus of $m = 4$ was chosen from theoretical analysis, and it was also used to minimize the sample size effects.

In the survey of the literature for the present study, datasets consisting of the average strength ($\langle\sigma\rangle$), standard deviation (S), Weibull modulus (m), and sample counts (N) have been collected. This kind of dataset is to be referred to as type V for values. When more than 10 strength values of comparable samples were available, either in numerical or graphical form, the data was digitized and analyzed. This kind will be called type D for digitized data, and the Weibull modulus will be determined using the basic method with simple linear regression available in Microsoft Excel[®]. The collected datasets will be presented in five groups. These are (1) historic iron and steel, (2) metals, (3) ceramics and glasses, (4) fibers, and (5) composite materials in tabular form. The tables have the following columns: material identification; $\langle\sigma\rangle$; S ; $\langle\sigma\rangle/S$; observed m value, m_{obs} ; estimated m value from Equation (14) given below, m_{est} ; N ; the ratio of m_{obs} to m_{est} ($= m_{obs}/m_{est}$); data type (V or D); note; and reference number.

Before the datasets were separated into five tables for publication, all 267 datasets were in a single file, and the constant for a trial approximation equation was varied to achieve the average value of the ratio of m_{obs} to m_{est} that was closest to unity. First, Equations (9) and (10) were used as trial functions, since both are equivalent to Equation (5). When these are inserted, the average values of m_{obs}/m_{est} (standard deviation in parentheses) were 0.948 (0.091) and 0.874 (0.083), respectively. These produced 5.2% and 12.6% error, indicating that the theoretical values are not suitable to represent experimental m values. Actual m values contain errors from various sources that have not been anticipated in theory. Next, the constant of linear Equation (10) was reduced to 1.2, 1.11, 1.10, and 1.09; the results are shown in Table 1. The constant of 1.11 gave the closest value of 1.001, while it increased to 1.01 using 1.10. The previously used constant of 1.2 (Equation (7)) resulted in $m_{obs}/m_{est} = 0.926$ or 7.4% error. Next, one-parameter power-law equations were inserted starting with Equation (8), changing the exponent to 1.05, 1.045, and 1.04, showing the results in Table 1. The exponent of 1.045 gave a value of 1.001 (0.095). This is comparable to the linear Equation with the constant of 1.11. Between the two groups giving similar matches in predicting m values from $\langle\sigma\rangle$ and S values, a simpler linear equation is preferable. Furthermore, the constant of 1.1 is selected as it provides a good fit and ease of use as well. This is given as Equation (14):

$$m = 1.10 \langle\sigma\rangle/S. \quad (14)$$

This will be called the modified Robinson relation hereafter. This was selected since it is linear and produced nearly the unity m_{obs}/m_{est} value (off by 1%) with a constant of two digits. Obviously, one can use 1.11 as the constant, but a different data population shifts the degree of agreement by 1% to 3%, as will be seen below. It is an approximate relation to represent observed Weibull moduli. It should be recalled that theoretically exact relationships are worse by 4% to 12%.

Table 1. Equation parameters and fit to experimentally observed m values.

Model Equation	Constant	Exponent	Average Ratio	Standard Deviation
Equation (10)	1.271	1.00	0.874	0.083
Equation (7)	1.20	1.00	0.926	0.082
Linear Equation	1.11	1.00	1.001	0.089
Linear Equation	1.105	1.00	1.005	0.089
Equation (14)	1.10	1.00	1.010	0.090
Linear Equation	1.095	1.00	1.014	0.090
Linear Equation	1.00	1.00	1.111	0.099
Equation (9)	1.0461	1.049	0.948	0.091
Equation (8)	1.00	1.064	0.958	0.098
Power Law Equation	1.00	1.050	0.990	0.083
Power Law Equation	1.00	1.045	1.001	0.095
Power Law Equation	1.00	1.040	1.012	0.095

The collective datasets are plotted in Figures 2 and 3 to show general behavior. Since 267 sets are included, most points overlapped, especially for lower $\langle\sigma\rangle/S$ values. In Figure 2, red + symbols represent m_{obs} and blue dots represent m_{est} , against $\langle\sigma\rangle/S$ values. Both symbols follow a single straight line. Figure 3 illustrates the deviation of measured m_{obs} values from the linear estimates of Equation (14) using m_{obs}/m_{est} . Most data points are within ± 0.1 (or $\pm 10\%$) of the unity ratio, with 11 points outside of ± 0.2 . For the collective dataset, the average of m_{obs}/m_{est} is 1.01, and the standard deviation is 0.09, justifying the selection of the constant, 1.1, which is used in Equation (14). Note that the corresponding average m_{obs}/m_{est} increases to 1.111 (0.099) for the simplest $m_{est} = \langle\sigma\rangle/S$ expression. This may be useable for getting a rough idea of m values.

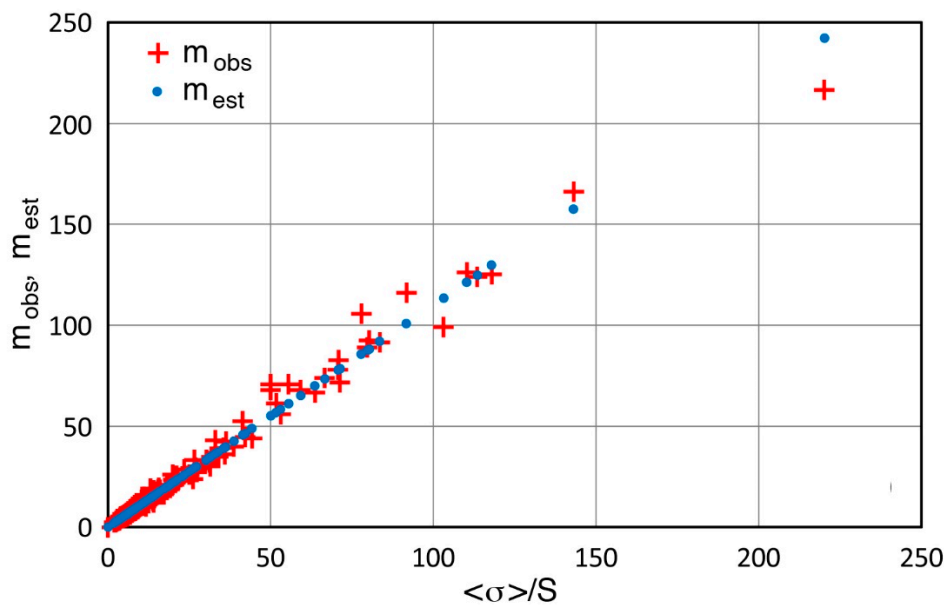


Figure 2. Plots of m_{obs} (red + symbol) and m_{est} (blue dot) vs. $\langle\sigma\rangle/S$ for the whole datasets.

4.1. Historic Wrought Iron and Steel

Table 2 lists the data of wrought iron and steel from the 19th century to the early 20th century. These are arranged roughly in the order of age. For these datasets, the average of m_{obs}/m_{est} is 1.007 and the standard deviation is 0.106, showing a similar deviation and a slightly larger standard deviation than the whole dataset. All the m_{obs} data in this group, except for the last five, were calculated from digitized strength data from the literature. Figure 4a shows the values of m_{obs} and m_{est} against $\langle\sigma\rangle/S$, as shown in Figure 2. Again, the m_{obs} values straddle the blue dots for m_{est} from Equation (14).

Figure 4b represents the deviation from the unity line. This figure is apparently skewed upward, but these are balanced by overlapping points below the unity line. This group also has the two lowest m_{obs}/m_{est} , which are below 0.8, balancing the high values.

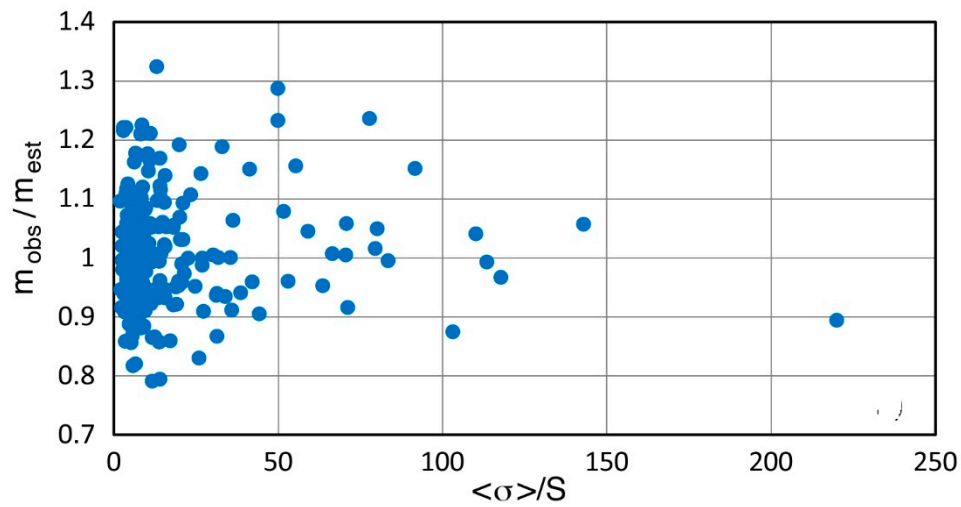


Figure 3. Plot of m_{obs}/m_{est} (blue dot) vs. $\langle\sigma\rangle/S$ for the whole datasets.

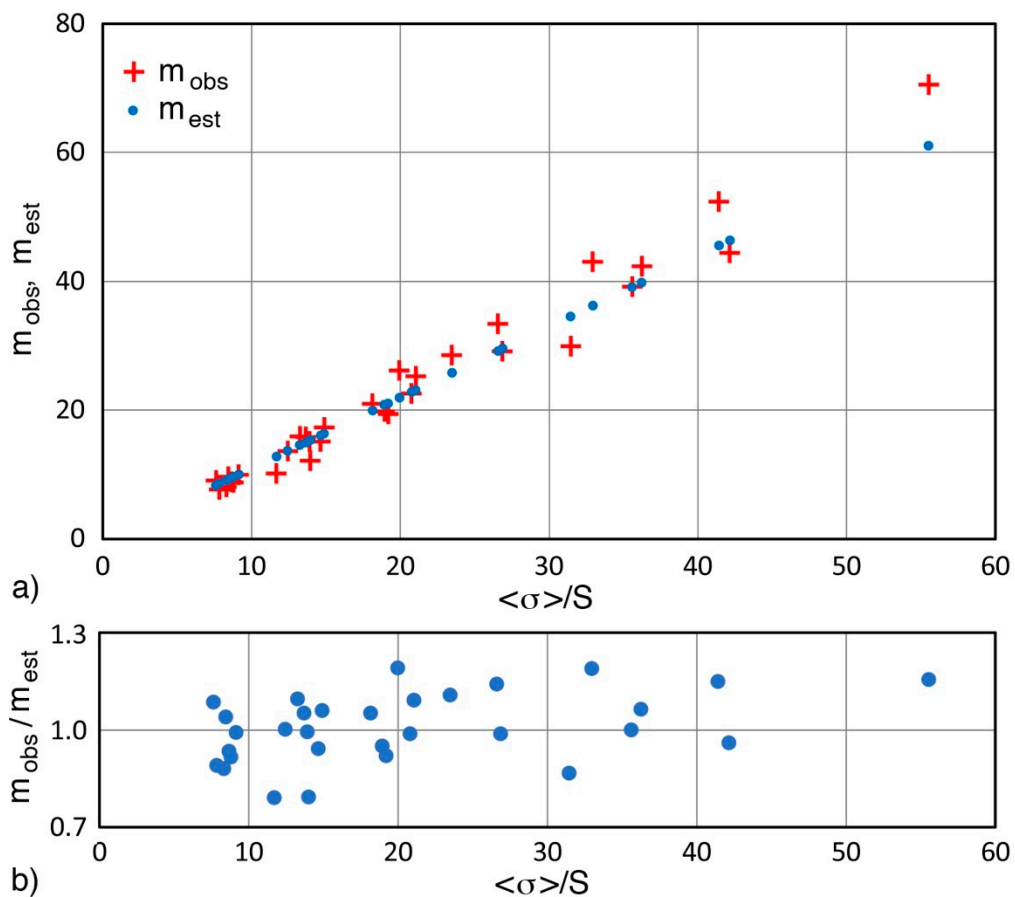


Figure 4. (a) Plots of m_{obs} (red + symbol) and m_{est} (blue dot) vs. $\langle\sigma\rangle/S$ for the historical iron and steel datasets. (b) Plot of m_{obs}/m_{est} (blue dot) vs. $\langle\sigma\rangle/S$ for the same.

Table 2. Listing of data for wrought iron and steel of the 19th century to the early 20th century.

Historical Iron/Steel	$\langle\sigma\rangle$	S	$\langle\sigma\rangle/SD$	m_{obs}	m_{est}	N	m_{obs}/m_{est}	Note	D/V	Ref
Finley 1810	338.0	40.54	8.34	8.08	9.17	26	0.881	Wrought iron	D	[34]
Franklin Inst 1837	369.9	31.66	11.68	10.16	12.85	11	0.791	Wrought iron	D	[35]
Franklin Inst 1837	358.7	40.86	8.78	8.85	9.66	11	0.916	Wrought iron	D	[35]
Franklin Inst 1837	354.9	40.89	8.68	8.92	9.55	36	0.934	Wrought iron	D	[36]
Kirkaldy Book 1862	425.6	20.21	21.06	25.3	23.16	32	1.092	Yorkshire from three works	D	[37]
Kirkaldy Book 1862	377.6	27.14	13.91	15.2	15.30	24	0.993	Consett Best long	D	[37]
Kirkaldy Book 1862	582.4	39.06	14.91	17.39	16.40	12	1.060	Naylor cast steel	D	[37]
Kirkaldy Book 1862	401.0	12.17	32.95	43.07	36.24	16	1.188	Govan Ex B best	D	[37]
Kirkaldy Book 1862	362.5	11.52	31.47	29.99	34.61	17	0.866	1860 Swedish iron	D	[35]
Kirkaldy Book 1862	406.1	17.29	23.49	28.6	25.84	16	1.107	Bradley charcoal iron	D	[37]
Kirkaldy Book 1862	382.4	48.76	7.84	7.69	8.63	325	0.892	Thick bar > 0.7"	D	[37]
Kirkaldy Book 1862	339.7	40.28	8.43	9.65	9.28	363	1.040	Thin bar < 0.7"	D	[37]
Indiana bridges	329.3	18.14	18.15	21	19.97	19	1.052	Bridge eyebar 1869	D	[38]
Indiana bridges	322.9	17.04	18.95	19.8	20.84	16	0.950	Bridge rod 1873	D	[38]
Indiana bridges	326.4	15.71	20.78	22.6	22.85	14	0.989	Low values cut off	D	[38]
Beardslee (US Navy) 1879	371.1	18.59	19.96	26.15	21.96	846	1.191	1879 whole data	D	[39]
Beardslee (US Navy) 1879	362.1	9.99	36.25	42.39	39.87	580	1.063	High values cut off	D	[39]
Beardslee (US Navy) 1879	391.7	14.57	26.88	29.2	29.57	456	0.988	Low values cut off	D	[39]
Beardslee (US Navy) 1879	390.8	20.36	19.20	19.44	21.12	69	0.921	Small diameter	D	[39]
Late 19c US sources	339.0	37.01	9.16	9.99	10.08	16	0.991	Wrought iron	D	[36]
Holley 1877	314.9	23.03	13.67	15.83	15.04	8	1.052	Wrought iron	D	[35]
Unwin 1910	473.5	11.23	42.16	44.5	46.38	14	0.959	Bessemer steel, 1880s	D	[40]
Unwin 1910	332.7	22.70	14.66	15.2	16.12	21	0.943	Boiler plate, 1880s	D	[40]
Unwin 1910	345.8	9.71	35.61	39.2	39.17	17	1.001	Boiler plate, 1880s	D	[40]
Unwin 1910	550.7	39.40	13.98	12.2	15.37	12	0.794	Steel Rail, 1880s	D	[40]
Percy 1886	1092.0	87.8	12.44	13.7	13.68	35	1.001	1886 patented wire	D	[41]
Williamsburg Br 1903	1499.0	113	13.27	16	14.59	160	1.096	1903 cable wire	D	[42]
534 repopt Br wires	1649.0	29.7	55.52	70.6	61.07	20	1.156	Stage 1,2 corrosion	V	[23]
534 repopt Br wires	1628.0	39.3	41.42	52.4	45.57	15	1.150	Stage 3 corrosion	V	[23]
534 repopt Br wires	1595.0	60	26.58	33.4	29.24	15	1.142	Stage 4 corrosion	V	[23]
534 repopt Br wires	1383.0	181.5	7.62	9.1	8.38	15	1.086	Stage 4 with cracks	V	[23]
Mid-Hudson Br	1609.1	51.66	31.15	32.07	34.26	NA	0.936	Stage 2,3 corrosion	V	[43]

D/V stands for data type of D = digitized and V = Values from the literature. Ref = reference number. Br = bridge. $\langle\sigma\rangle$ = average strength. S = standard deviation. $\langle\sigma\rangle/S$; mobs = observed Weibull modulus value. Mest = estimated m value from Equation (14). N = sample counts.

The first row in Table 2 gives the results of 1810 chain links that were retrieved from the Essex-Merrimack suspension bridge when it was replaced in 1910 [34,35]. This was built by James Finley, and was one of the earliest iron suspension bridges in the West. The strength level was high for its age, but the m values were below 10, which was indicative of the brittle state expected of such an old iron. In this case, tests were done on materials after 100 years of continuous use outdoors. The next three rows provide the results of tests conducted at the Franklin Institute in 1837 [35,36]. Both strength and m values are comparable to the Finley iron. The next eight rows show the test data from Kirkaldy's 1863 book [37]. The selected six groups are given first, grouping the same or related sources of best quality iron, cast steel, and charcoal iron. One group that was noted as "Govan Ex Best" produced a high m value of 43, while cast steel had a high strength (580 MPa) and an m value of 17. Gordon selected the data of coveted Swedish iron from Kirkaldy [35,37], which gives an m value of 30, justifying its high reputation. The next row, which is noted as charcoal iron, may also be of Swedish origin. The following two rows represent most of Kirkaldy's iron and steel data, totaling 688 tests. These data were tabulated in [38] and were split into two groups by sample diameters. The smaller diameter group had 40 MPa higher strength, but both had low m values of ~ 9 , as low-quality iron samples were included. These two datasets represent the general quality level of 1860 iron in the United Kingdom (UK).

The next three rows give data from two Indiana bridges (built in 1869 and 1873) [38]. By this time, m values had doubled from the Finley iron, indicating the quality improvement of iron available in the United States (US) Midwest. Beardslee [39] conducted extensive testing at the US Navy, reporting 846 test results in 1879. For the entire tests, an m value of 26 was comparable to Indiana bridge irons, but the strength was 50 MPa higher. When the data were separated into low-strength and high-strength groups (with overlaps), the m value rose to 42 for the low group, which was comparable to the best data from the 1860 UK, albeit with 30 MPa lower strength. However, a general sampling of US wrought iron still showed the presence of low-quality iron with m values of approximately 10 to 15, as shown by Gordon [35,36]. By the 1880s, steel was widely used, and Unwin's book provided four examples of better materials [40]. These included Bessemer steel, boiler plates, and railroad rail.

The last seven rows give the data for patented high strength steel wires, mainly for suspension bridge cables. Percy's article [41] reported UK test results in the 1880s. The strength reached a level of 1 GPa, but the m value was still 13.7 [15,44]. At about the same time, wires for the Brooklyn Bridge (finished in 1883) had the strength of 1.1 GPa. Unfortunately, no test data has been located so far. Over the next 20 years, steel technology improved further and provided 1.5-GPa steel wires for the Williamsburg Bridge in New York (finished in 1903). Perry [42] provided 160 test data for the cable wires that were removed during the rehabilitation work in the 1980s, and Weibull analysis was conducted [15,44], yielding $m = 16$ with an average tensile strength of 1.5 GPa. The values are remarkable after more than 80 years of use, since these wires did not have galvanizing protection against corrosion. The next four datasets were commented on earlier in the Introduction [23], while the last set was from the Mid-Hudson Bridge [43]. These wires were from suspension bridges after many years of service. As noted before, m values are indicative of the state of corrosion of the suspension cable wires, and are useful in assessing the remaining service life of suspension cables. There are also many historic wrought iron bridges in need of rehabilitation, and simple Weibull analysis, which is being discussed here, will be helpful in their evaluation.

4.2. Metals and Alloys

Table 3 lists the data of metals and alloys. For these datasets, the average of $m_{\text{obs}}/m_{\text{est}}$ is 1.034, and the standard deviation is 0.093. The $m_{\text{obs}}/m_{\text{est}}$ average is 2.4% higher than that for the whole set. This comes partly from 11 data points with $m_{\text{obs}}/m_{\text{est}} > 1.1$, but these large deviations are still within the expected behavior. Most metallic alloys exhibit good ductility, and Weibull analysis is usually not needed. It is often assumed that metal alloys have m values of over 100, but lower m values have been obviously observed. The top four rows are calculated from the results of the ASTM study at established

laboratories in the United States [24], and the m values were 74 to 124 (Figure 1), as discussed in Section 3 above. The data for Nimonic[®] 75 Ni-base alloy from the European interlaboratory study [25] yielded $m = 125$ (Figure 1). Here, another Ni alloy, Inconel[®] 625 (American Special Metals, Miami, FL, USA) showed $m = 55$ [45]. These six datasets can be treated as the benchmarks for ductile steel, Al alloys, and Ni alloys. It is important to recognize that these studies used well-controlled sets of samples. This approach is usually replicated in research laboratories, but it is not representative of large sample data for design and reliability works, where mill practice, alloy chemistry, and structural shapes vary (see Section 5.2 for more discussion). Weibull data for metals and alloys are indeed scarce, and 22 of the 43 datasets in Table 3 showed $m > 50$. These were all ductile metals and alloys, including 18Ni maraging steel, stainless steels, and Mg alloys. However, some ductile metals such as copper showed low m values of 12 to 16 as well. Sintered steel showed low ductility along with low m values below 30. More data with low m values are given in Section 5 using standard deviation (or CV), where one finds that $m < 30$ is common for large-scale industrial datasets. Brittle fracture data for steels at sub-zero temperatures should be assessed using Weibull analysis, but even here, the test results of repeated tests are difficult to find. Several datasets for cleavage fracture were analyzed and added to Table 3 at rows 9 to 12 [46]. Surprisingly, m values were 10 to 20 in a sharp contrast to the theoretical value of 4 predicted by Wallin [32,33]. Another brittle material is nickel aluminide (NiAl). Monocrystalline NiAl showed consistently low m values of about 5 [47], while NiTi intermetallic showed a slightly higher m of 8.5 [46]. General trends can be viewed in Figure 5. No peculiar behavior is present.

Table 3. Listing of data for metals and alloys.

Metals and Alloys	$\langle\sigma\rangle$	S	$\langle\sigma\rangle/SD$	m_{obs}	m_{est}	N	m_{obs}/m_{est}	Note	D/V	Ref
Al 6061	396.2	3.49	113.52	124.00	124.88	30	0.993	ASTM E28 study	D	[24]
Al 7075	611.2	7.3	83.50	91.40	91.85	30	0.995	ASTM E28 study	D	[24]
1018 steel	497.0	7.5	66.62	73.80	73.28	29	1.007	ASTM E28 study	D	[24]
4142 steel	1004.0	14.2	70.70	78.10	77.77	30	1.004	ASTM E28 study	D	[24]
Nimonic® 75	750.8	6.4	117.86	125.30	129.65	18	0.966	European study	D	[25]
Inconel® 625	886.3	16.5	53.72	54.70	59.09	21	0.926	production plates	D	[45]
Copper-oxygen free	226.2	21.1	10.73	11.96	11.80	33	1.013	annealed	D	[48]
Copper-oxygen free	427.0	29.8	14.34	15.88	15.78	22	1.006	cold worked 90%	D	[48]
Steel coarse carbides	1599.0	77.0	20.77	21.87	22.84	10	0.957	Cleavage fracture	D	[46]
WCF62 steel at $-196\text{ }^{\circ}\text{C}$	1257.0	118.4	10.62	13.40	11.68	13	1.147	Cleavage fracture	D	[46]
C-Mn steel at $-100\text{ }^{\circ}\text{C}$	1787.0	116.0	15.41	18.54	16.95	20	1.094	Cleavage fracture	D	[46]
C-Mn steel Quenched	58.9	6.8	8.69	10.68	9.56	16	1.118	K_{Ic} at $-100\text{ }^{\circ}\text{C}$	D	[46]
Stainless steel 430	507.4	9.6	53.08	56.03	58.38	12	0.960	Annealed	V	[49]
Stainless steel 316L	636.9	10.0	63.62	66.62	69.98	20	0.952	Annealed	V	[49]
Stainless steel 301HT	1649.0	23.1	71.29	71.79	78.42	26	0.915	Cold rolled	V	[49]
0.4C-1.5Cr-1.5Ni steel	644.0	45.0	14.31	17.56	15.74	25	1.115	Sintered steel	V	[50]
0.4C-1.5Cr-1.5Ni steel	622.0	25.0	24.88	26.04	27.37	24	0.951	Sintered steel	V	[50]
0.4C-1.5Cr-1.5Ni steel	508.0	36.0	14.11	17.41	15.52	24	1.122	Sintered steel	V	[50]
0.4C-1.5Cr-1.5Ni steel	728.0	50.0	14.56	16.15	16.02	25	1.008	Sintered steel	V	[50]
0.4C-1.5Cr-1.5Ni steel	710.0	35.0	20.29	23.01	22.31	25	1.031	Sintered steel	V	[50]
0.4C-1.5Cr-1.5Ni steel	669.0	43.0	15.56	19.50	17.11	24	1.139	Sintered steel	V	[50]
18Ni Maraging steel	1147.3	11.1	103.17	99.20	113.49	9	0.874	laser sintered	D	[51]
ZM61 Mg alloy Extruded	210.3	1.5	143.06	166.30	157.37	20	1.057	Yield strength	V	[52]
ZM61 Mg alloy Extruded	285.7	3.6	80.25	92.60	88.28	20	1.049	Fracture strength	V	[52]
ZM61 Mg alloy Extruded	303.8	1.4	220.14	216.40	242.16	20	0.894	Tensile strength	V	[52]
ZM61 Mg alloy Aged	312.3	3.9	79.67	89.00	87.64	20	1.016	Yield strength	V	[52]
ZM61 Mg alloy Aged	312.8	9.2	33.89	34.80	37.28	20	0.934	Fracture strength	V	[52]
ZM61 Mg alloy Aged	349.6	3.2	110.28	126.20	121.31	20	1.040	Tensile strength	V	[52]
AE44 Mg alloy	243.7	7.7	31.73	34.90	34.90	15	1.000	Tested at 295 K	D	[53]
AE44 Mg alloy	159.6	7.0	22.74	25.00	25.01	5	1.000	Tested at 394 K	D	[53]
Al-Si casting alloy	195.4	3.8	51.69	61.30	56.86	52	1.078	Sand mould: modified	D	[54]
Al-Si casting alloy	188.3	3.2	59.22	68.03	65.15	50	1.044	Metal mould	V	[54]
Al-Si casting alloy	215.9	3.0	70.93	82.58	78.03	50	1.058	Metal mould: modified	V	[54]
Al-Si casting alloy	192.5	3.9	50.00	67.80	55.00	50	1.233	Sand mould, heat treat	V	[54]
Al-Si casting alloy	207.6	4.2	50.02	70.80	55.03	50	1.287	Metal mould, heat treat	V	[54]

Table 3. *Cont.*

Metals and Alloys	$\langle\sigma\rangle$	S	$\langle\sigma\rangle/SD$	m_{obs}	m_{est}	N	m_{obs}/m_{est}	Note	D/V	Ref
Al–Si casting alloy	221.8	2.9	77.82	105.80	85.61	50	1.236	Sand, heat treat, modified	V	[54]
Al–Si casting alloy	235.3	2.6	91.73	116.20	100.91	50	1.152	Metal, heat treat, modified	V	[54]
NiAl single crystal	1261.0	209.0	6.03	6.10	6.64	15	0.919	Brittle fracture	V	[47]
NiAl single crystal	1010.0	202.0	5.00	5.40	5.50	32	0.982	Brittle fracture	V	[47]
NiAl single crystal	767.0	177.0	4.33	4.80	4.77	9	1.007	Brittle fracture	V	[47]
NiAl single crystal	629.0	130.0	4.84	5.50	5.32	15	1.033	Brittle fracture	V	[47]
NiAl single crystal	470.0	109.0	4.31	5.30	4.74	13	1.117	Brittle fracture	V	[47]
NiTi intermetallic	440.0	56.8	7.75	8.81	8.53	14	1.033	Brittle fracture	D	[46]

D/V stands for data type of D = digitized and V = Values from the literature. Ref = reference number.

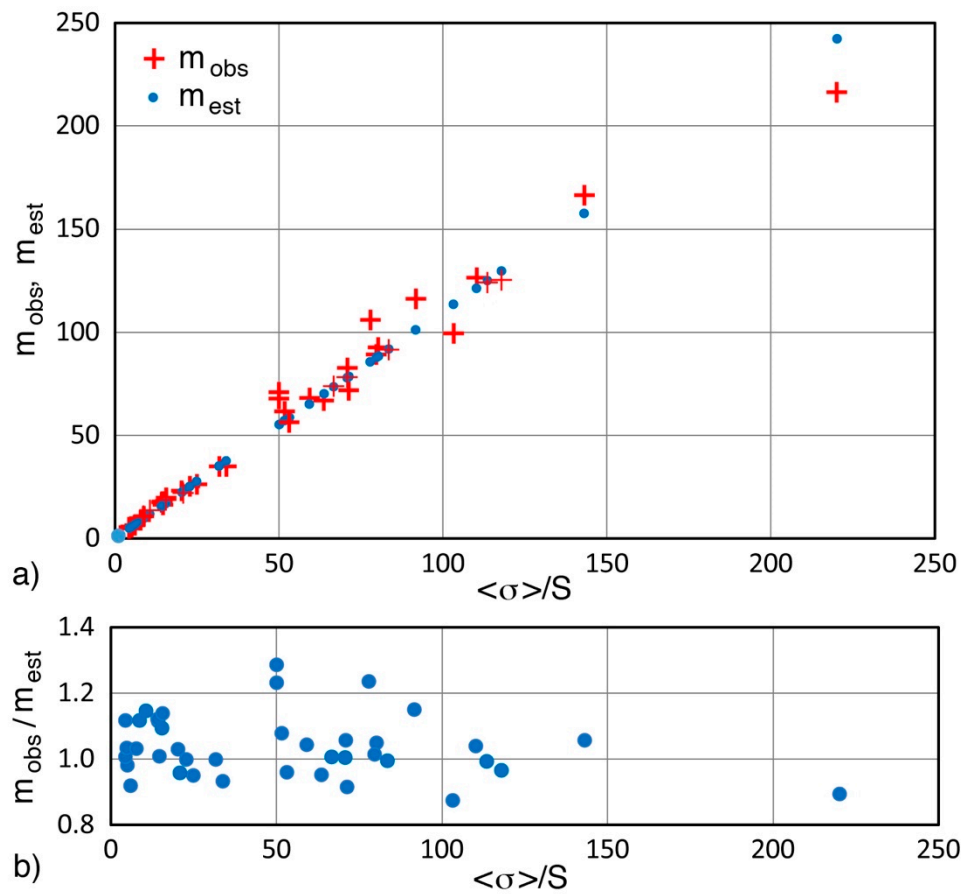


Figure 5. (a) Plots of m_{obs} (red + symbol) and m_{est} (blue dot) vs. $\langle\sigma\rangle/S$ for the metal data. (b) Plot of m_{obs}/m_{est} (blue dot) vs. $\langle\sigma\rangle/S$ for the same.

4.3. Ceramics and Glasses

Table 4 lists the data of ceramics and glasses. For these datasets, the average of m_{obs}/m_{est} is 1.011, and the standard deviation is 0.100. These values are similar to those of the whole set, while the general trends seen in Figure 6a,b resemble those of historic iron and steel. That is, more deviations larger than ± 0.1 exist. The maximum m value is limited to 24, and larger m values are found for high-performance ceramics such as alumina, porcelain, silicon nitride, and stabilized zirconia [47,55,56]. In the strength testing of these brittle materials, Weibull analysis is included as a rule, and many reports are available. However, the average and standard deviation data are left out from many test reports. In fact, Equation (7) is used to get CV values from m in ASTM C1499 [26]. This omission of $\langle\sigma\rangle$ and S precluded such tests from this study, unfortunately.

Table 4. Listing of data for ceramics and glasses.

Ceramics and Glasses	$\langle\sigma\rangle$	S	$\langle\sigma\rangle/SD$	m_{obs}	m_{est}	N	m_{obs}/m_{est}	Note	D/V	Ref
Almina (99.8%)	306.9	21.4	14.36	17.40	15.80	33	1.101	Flexure strength	V	[57]
Almina (98%-Corbit98)	240.7	68.6	3.51	3.31	3.86	10	0.858	Brazilian split test	D	[58]
Almina (98%-Corbit98)	341.5	56.1	6.09	5.95	6.70	8	0.889	Brazilian split test	D	[58]
Sapphire single crystal	703.0	242.0	2.90	3.40	3.20	8	1.064	c-plane	V	[59]
Sapphire single crystal	1061.0	372.0	2.85	3.41	3.14	8	1.087	c-plane	V	[59]
Sapphire single crystal	427.0	118.0	3.62	4.09	3.98	6	1.028	r-plane	V	[59]
Sapphire single crystal	595.0	150.0	3.97	4.10	4.36	12	0.940	r-plane	V	[59]
WC cermet	2910.0	223.0	13.05	19.00	14.35	29	1.324	8% Ni binder	V	[47]
ZrO ₂ -TiB ₂	1124.0	177.0	6.35	7.10	6.99	22	1.016	Flexure strength	V	[60]
ZrO ₂	860.3	343.5	2.50	2.81	2.76	33	1.020	Flexure strength	V	[60]
Si ₃ N ₄	614.4	173.9	3.53	4.04	3.89	18	1.040	Fracture strength	V	[60]
Glass	61.7	6.8	9.05	10.32	9.95	40	1.037	Fracture strength	D	[60]
Soda Lime Glass	119.7	20.6	5.82	5.74	6.40	24	0.897	Fracture strength	V	[55]
Si ₃ N ₄	899.4	80.5	11.17	14.89	12.29	55	1.211	Fracture strength	V	[55]
SiC	357.9	42.3	8.47	9.62	9.32	75	1.033	Fracture strength	V	[55]
ZnO	102.4	5.2	19.80	20.92	21.78	109	0.960	Fracture strength	V	[55]
Si ₃ N ₄	875.9	76.2	11.49	12.55	12.64	30	0.993	3pt bend flexure strength	D	[61]
Si ₃ N ₄	733.3	77.7	9.43	10.42	10.38	27	1.004	4pt bend flexure strength	D	[61]
Si ₃ N ₄	689.6	63.9	10.79	12.16	11.87	31	1.024	Biaxial test	D	[61]
Porcelain CM	86.3	4.3	20.07	23.60	22.08	30	1.069	Dental ceramics	V	[56]
Glass ceramic D	70.3	12.2	5.76	5.50	6.34	30	0.868	Dental ceramics	V	[56]
Alumina-porcelain ICA	429.3	87.2	4.92	5.70	5.42	30	1.053	Dental ceramics	V	[56]
Leucite-porcelain IE	83.9	11.3	7.42	8.60	8.17	30	1.053	Dental ceramics	V	[56]
Alumina-feldspar-porcelain	131.0	9.5	13.79	13.00	15.17	30	0.857	Dental ceramics	V	[56]
Feldspar-porcelain VAD	60.7	6.8	8.93	10.00	9.82	30	1.018	Dental ceramics	V	[56]
Feldspar-porcelain VMK	82.7	10.0	8.27	8.90	9.10	30	0.978	Dental ceramics	V	[56]
Partially stabilized Zirconia	913.0	50.2	18.19	18.40	20.01	30	0.920	Dental ceramics	V	[56]
Fused quartz	109.0	14.0	7.79	8.82	8.56	28	1.030	25mm diameter	V	[62]
Fused quartz	102.0	11.0	9.27	10.60	10.20	25	1.039	75 mm diameter	V	[62]
Fused quartz	77.7	13.2	5.89	6.08	6.48	23	0.939	225 mm diameter	V	[62]
Fused quartz	172.0	20.0	8.60	10.20	9.46	11	1.078	25 mm repolished	V	[62]
Alumina	364.0	45.0	8.09	9.60	8.90	32	1.079	4pt bend flexure strength	V	[63]
Alumina	444.0	51.0	8.71	8.80	9.58	30	0.919	3pt bend flexure strength	V	[63]
Porcelain	84.7	5.3	15.98	18.50	17.58	27	1.052	4pt bend flexure strength	V	[63]
Porcelain	112.0	8.0	14.00	18.00	15.40	26	1.169	4pt bend flexure strength	V	[63]

Table 4. Cont.

Ceramics and Glasses	$\langle\sigma\rangle$	S	$\langle\sigma\rangle/SD$	m_{obs}	m_{est}	N	m_{obs}/m_{est}	Note	D/V	Ref
Porcelain	57.0	3.6	15.66	16.30	17.23	30	0.946	porcelain glazed	V	[64]
Porcelain	52.0	5.3	9.77	10.50	10.75	30	0.977	1000 grit polish	V	[64]
Porcelain	48.0	4.7	10.28	13.30	11.31	30	1.176	600 grit polish	V	[64]
Porcelain	46.2	4.7	9.89	10.80	10.88	30	0.992	100 grit polish	V	[64]
Zirconia	757.0	79.0	9.58	11.40	10.54	40	1.082	Maximum likelihood	V	[65]
Zirconia	1077.0	113.0	9.53	9.60	10.48	40	0.916	Maximum likelihood	V	[65]
Zirconia	891.0	115.0	7.75	9.40	8.52	40	1.103	Maximum likelihood	V	[65]
Zirconia	1126.0	114.0	9.88	10.30	10.86	40	0.948	Maximum likelihood	V	[65]
Zirconia	835.0	102.0	8.19	10.90	9.00	40	1.210	Maximum likelihood	V	[65]
Zirconia	1322.0	214.0	6.18	7.90	6.80	40	1.163	Maximum likelihood	V	[65]
Graphite	19.1	1.7	11.38	11.54	12.51	108	0.922	NBG18 Graphite	V	[66]
Graphite	21.1	1.6	13.35	14.77	14.68	140	1.006	NBG18 Graphite	V	[66]
Graphite	18.9	1.8	10.44	10.73	11.49	56	0.934	NBG18 Graphite	V	[66]
Dental Ceramic E1	84.5	14.6	5.79	5.20	6.37	20	0.817	Flexure strength	V	[67]
Dental Ceramic E2	215.0	40.1	5.36	5.40	5.90	20	0.916	Flexure strength	V	[67]
Dental Ceramic ES	239.0	36.3	6.58	7.20	7.24	20	0.994	Flexure strength	V	[67]
Dental Ceramic GV	63.8	5.8	11.00	14.10	12.10	20	1.165	Flexure strength	V	[67]
Dental Ceramic ES-G	231.0	45.0	5.13	5.00	5.65	20	0.885	Flexure strength	V	[67]
Dental Ceramic ES-GV-G	238.0	40.5	5.88	6.10	6.46	20	0.944	Flexure strength	V	[67]
Dental Ceramic ES	285.0	48.9	5.83	6.20	6.41	20	0.967	Flexure strength	V	[67]
Hydroxyapatite	110.0	18.5	5.95	5.82	6.54	30	0.890	Flexure strength	V	[68]
Hydroxyapatite	18.6	2.5	7.44	7.24	8.18	30	0.885	Flexure strength	V	[68]
Hydroxyapatite	70.9	8.8	8.06	8.67	8.86	30	0.978	Compression	V	[68]
Hydroxyapatite	21.8	2.3	9.48	10.30	10.43	30	0.988	Compression	V	[68]
Hydroxyapatite	91.0	16.0	5.69	6.80	6.26	20	1.087	1360 °C 240 min	V	[69]
Hydroxyapatite	69.0	10.0	6.90	8.40	7.59	24	1.107	1360 °C 12 min	V	[69]

D/V stands for data type of D = digitized and V = Values from the literature. Ref = reference number

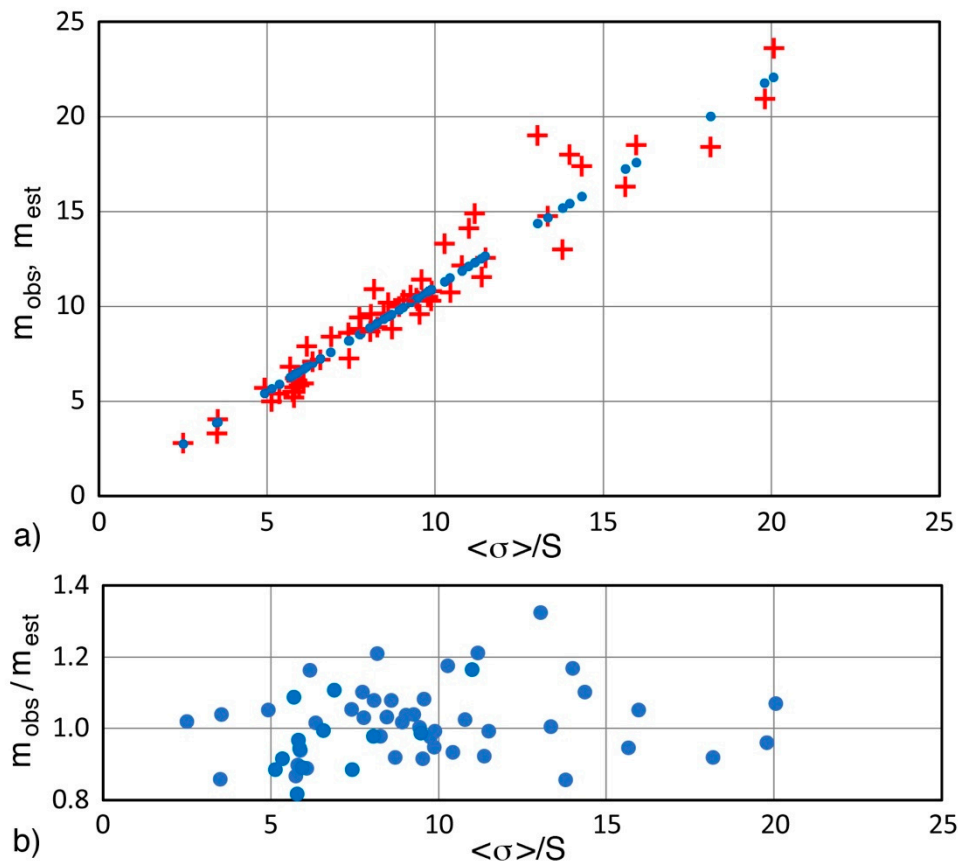


Figure 6. (a) Plots of m_{obs} (red + symbol) and m_{est} (blue dot) vs. $\langle\sigma\rangle/S$ for the data of ceramics and glasses. (b) Plot of m_{obs}/m_{est} (blue dot) vs. $\langle\sigma\rangle/S$ for the same.

4.4. Fibers

Table 5 lists the data of fibers, which constitute the largest group in this Weibull modulus survey. Datasets for over 90 types of fibers have been collected. About half of them are for carbon fibers, reflecting the high interest in their properties. For these datasets, the average of m_{obs}/m_{est} is 1.007, and the standard deviation is 0.072. The value of m_{obs}/m_{est} is close to unity. Data trends on Figure 7 show less data scatters than other similar plots. This trend is better seen in Figure 7b, and less than 20% of the data points showed a deviation higher than ± 0.1 . The m values are confined to a range of 2 to 11, implying more brittle behavior even compared to ceramics, and reflecting the higher strength levels of fibers. Only four datasets exceeded $m \approx 10$ [70–72]. Natural fibers included showed mostly low m values below 5, while those above 8 were either carbon or ceramic fibers made in recent years. Data for glass fibers became scarce after the 1970s, while early data lacked some of the parameters that were needed here, and only 10 datasets were found. Again, reported Weibull modulus studies often omitted $\langle\sigma\rangle$ and S data.

Table 5. Listing of data for fibers.

Fibers	$\langle\sigma\rangle$	S	$\langle\sigma\rangle/SD$	m_{obs}	m_{est}	N	m_{obs}/m_{est}	Note	D/V	Ref
E-glass fiber	811.5	130.8	6.20	6.54	6.82	33	0.958	GE fiber 1963	D	[11]
Silica fiber	1199.8	636.8	1.88	2.27	2.07	119	1.095	1060 mm gage length	D	[73]
S-glass fiber	5654.0	888.0	6.37	6.98	7.00	23	0.997	25.4 mm gage length	D	[74]
S-glass fiber	4507.0	954.0	4.72	5.39	5.20	23	1.037	3.17 mm gage length	D	[74]
Glass fiber	11,016.0	2367.0	4.65	4.54	5.12	15	0.887	Under ultra high vacuum	D	[75]
Glass fiber	1920.0	640.0	3.00	4.03	3.30	40	1.221	Water-based sizing	V	[76]
Glass fiber	2020.0	530.0	3.81	5.12	4.19	40	1.221	Sizing A1100	V	[76]
Glass fiber	1750.0	340.0	5.15	5.53	5.66	40	0.977	Sizing P122 1200 Tex	V	[76]
Glass fiber	1420.0	470.0	3.02	4.04	3.32	40	1.216	Sizing P122 2400 Tex	V	[76]
E-Glass fiber	1370.0	620.0	2.21	2.30	2.43	40	0.946	Tensile strength	V	[77]
C fiber HTS	2434.6	558.0	4.36	4.67	4.80	30	0.973	Tensile strength	V	[74]
C fiber HTS	2227.7	479.3	4.65	5.02	5.11	30	0.982	Tensile strength	V	[74]
C fiber HTS	2324.3	344.9	6.74	6.08	7.41	30	0.820	Tensile strength	V	[74]
C fiber HTS	2145.0	373.8	5.74	5.97	6.31	30	0.946	Tensile strength	V	[74]
C fiber HTS	2000.1	549.7	3.64	3.97	4.00	30	0.992	Tensile strength	V	[74]
C fiber HTS	1620.8	316.6	5.12	5.55	5.63	30	0.985	Tensile strength	V	[74]
C pitch fiber C130	4370.0	830.0	5.27	6.07	5.79	16	1.048	Tensile strength	V	[78]
C pitch fiber C130	3540.0	820.0	4.32	4.66	4.75	15	0.981	Tensile strength	V	[78]
C pitch fiber C130	3380.0	840.0	4.02	4.68	4.43	18	1.057	Tensile strength	V	[78]
C pitch fiber E700	4530.0	1110.0	4.08	4.81	4.49	16	1.071	Tensile strength	V	[78]
C pitch fiber E700	4230.0	960.0	4.41	4.82	4.85	19	0.994	Tensile strength	V	[78]
C pitch fiber E700	3670.0	840.0	4.37	4.88	4.81	12	1.015	Tensile strength	V	[78]
C fiber XN05	1100.0	150.0	7.33	7.90	8.07	20	0.979	Tensile strength	V	[79]
C fiber XN05	1438.0	283.0	5.08	5.41	5.59	20	0.968	Compressive strength	V	[80]
C fiberT1000GB	5690.0	1020.0	5.58	5.90	6.14	20	0.961	Tensile strength	V	[79]
C fiberT1000GB	894.0	139.0	6.43	6.86	7.07	20	0.970	Compressive strength	V	[80]
C fiber K13D	3210.0	810.0	3.96	4.20	4.36	20	0.963	Tensile strength	V	[79]
C fiber K13D	37.0	4.0	9.25	9.00	10.18	20	0.885	Compressive strength	V	[80]
C fiber T300	3200.0	490.0	6.53	7.00	7.18	20	0.974	Tensile strength	V	[79]
C fiber T300	857.0	140.0	6.12	6.80	6.73	20	1.010	Compressive strength	V	[80]
C fiber IM600	4390.0	790.0	5.56	5.87	6.11	20	0.960	Tensile strength	V	[79]
C fiber T700SC	4742.0	770.0	6.16	6.54	6.77	20	0.965	Tensile strength *	V	[80]
C fiber T700SC	959.0	169.0	5.67	6.14	6.24	20	0.984	Compressive strength	V	[80]
C fiber T800HB	5168.0	800.0	6.46	6.58	7.11	20	0.926	Tensile strength *	V	[80]
C fiber T800SC	5245.0	786.0	6.67	6.98	7.34	20	0.951	Tensile strength *	V	[80]

Table 5. Cont.

Fibers	$\langle\sigma\rangle$	S	$\langle\sigma\rangle/SD$	m_{obs}	m_{est}	N	m_{obs}/m_{est}	Note	D/V	Ref
C fiber T800HB	964.0	152.0	6.34	6.90	6.98	20	0.989	Compressive strength	V	[80]
C fiber M40B	2470.0	390.0	6.33	6.80	6.97	20	0.976	Tensile strength	V	[79]
C fiber M40B	807.0	113.0	7.14	7.81	7.86	20	0.994	Compressive strength	V	[80]
C fiber M60JB	3380.0	630.0	5.37	5.80	5.90	20	0.983	Tensile strength	V	[79]
C fiber M60JB	999.0	145.0	6.89	7.57	7.58	20	0.999	Compressive strength	V	[80]
C fiber TR50	4211.0	675.0	6.24	6.55	6.86	20	0.955	Tensile strength *	V	[80]
C fiber IMS60	5200.0	874.0	5.95	6.33	6.54	20	0.966	Tensile strength *	V	[80]
C fiber IMS60	711.0	114.0	6.24	6.84	6.86	20	0.997	Compressive strength	V	[80]
C fiber UM55	4733.0	857.0	5.52	5.83	6.08	20	0.960	Tensile strength *	V	[80]
C fiber UM55	502.0	66.0	7.61	8.34	8.37	20	0.997	Compressive strength	V	[80]
C fiber K135	3410.0	667.0	5.11	5.36	5.62	20	0.952	Tensile strength *	V	[80]
C fiber K135	87.0	11.0	7.91	9.00	8.70	20	1.034	Compressive strength	V	[80]
C fiber K13C	3270.0	826.0	3.96	4.21	4.35	20	0.967	Tensile strength *	V	[80]
C fiber K13C	35.0	4.0	8.75	9.22	9.63	20	0.958	Compressive strength	V	[80]
C fiber XN60	3326.0	626.0	5.31	5.63	5.84	20	0.964	Tensile strength *	V	[80]
C fiber XN60	91.0	11.0	8.27	9.10	9.10	20	1.000	Compressive strength	V	[80]
C fiber XN 90	3400.0	640.0	5.31	5.00	5.84	20	0.856	Tensile strength	V	[79]
C fiber XN 90	82.0	10.0	8.20	8.54	9.02	20	0.947	Compressive strength	V	[80]
Basalt fiber	1440.0	570.0	2.53	2.90	2.78	40	1.044	Tensile strength	V	[55]
Basalt fiber	1840.0	720.0	2.56	2.80	2.81	40	0.996	Homogenized	V	[55]
Nextel 610 fiber	3080.0	348.0	8.85	10.90	9.74	50	1.120	Tensile strength	V	[70]
Nextel 720 fiber	1964.0	287.0	6.84	8.10	7.53	50	1.076	Tensile strength	V	[70]
Nextel 720 fiber	1940.0	310.0	6.26	6.90	6.88	115	1.002	Tensile strength	V	[71]
Nextel 720 fiber	1880.0	300.0	6.27	6.87	6.89	53	0.997	Tensile strength	V	[71]
Nextel 720 fiber	1750.0	310.0	5.65	6.09	6.21	72	0.981	Tensile strength	V	[71]
Nextel 720 fiber	1710.0	220.0	7.77	8.90	8.55	50	1.041	Tensile strength	V	[71]
Nextel 720 fiber	1620.0	280.0	5.79	5.99	6.36	19	0.941	Tensile strength	V	[71]
Nextel 720 fiber	1428.0	168.0	8.50	10.30	9.35	51	1.102	Tensile strength	V	[71]
Nextel 720 fiber	1880.0	300.0	6.27	6.86	6.89	86	0.995	Tensile strength	V	[71]
SiCN fibers	952.0	254.0	3.75	4.57	4.12	50	1.108	Tensile strength	V	[81]
SiCN fibers	1001.0	256.0	3.91	4.46	4.30	50	1.037	Tensile strength	V	[81]
SiCN fibers	1113.0	223.0	4.99	6.02	5.49	50	1.097	Tensile strength	V	[81]
SiCN fibers	747.0	91.0	8.21	9.96	9.03	50	1.103	Tensile strength	V	[81]
SiCN fibers	1268.0	187.0	6.78	7.96	7.46	50	1.067	Tensile strength	V	[81]
SiCN fibers	802.0	110.0	7.29	8.86	8.02	50	1.105	Tensile strength	V	[81]

Table 5. Cont.

Fibers	$\langle\sigma\rangle$	S	$\langle\sigma\rangle/SD$	m_{obs}	m_{est}	N	m_{obs}/m_{est}	Note	D/V	Ref
Ni-metallic glass	1950.0	590.0	3.31	3.60	3.64	21	0.990	Tensile strength	V	[82]
Ni-metallic glass	1240.0	400.0	3.10	3.20	3.41	18	0.938	Tensile strength	V	[82]
Alumina fiber	2248.4	255.2	8.81	10.30	9.69	126	1.063	76 mm gage length	V	[72]
Alumina fiber	1751.8	400.0	4.38	4.50	4.82	46	0.934	254 mm gage length	V	[72]
SiC fiber	3924.4	648.3	6.05	6.34	6.30	74	1.006	76 mm gage length	V	[72]
SiC fiber	2965.7	648.3	4.57	4.97	4.90	65	1.014	254 mm gage length	V	[72]
SiC (Nicalon) fiber	3300.0	570.0	5.79	7.03	6.37	20	1.104	Flame desized	V	[83]
SiC (Nicalon) fiber	3190.0	730.0	4.37	5.41	4.81	20	1.125	Flame desized	V	[83]
SiC (Nicalon) fiber	2690.0	670.0	4.01	4.93	4.42	20	1.116	HF treated	V	[83]
SiC (Nicalon) fiber	3040.0	530.0	5.74	6.66	6.31	20	1.056	HF treated	V	[83]
SiC (Nicalon) fiber	2800.0	530.0	5.28	5.96	5.81	20	1.026	HF treated	V	[83]
SiC (Nicalon) fiber	2380.0	400.0	5.95	7.15	6.55	20	1.092	HF treated	V	[83]
Hemp fiber	268.1	38.5	6.97	8.29	7.66	20	1.082	0.4-mm diameter	V	[84]
Hemp fiber	222.1	55.7	3.98	4.52	4.38	20	1.031	0.5-mm diameter	V	[84]
Hemp fiber	150.3	34.4	4.37	5.01	4.81	20	1.041	0.6-mm diameter	V	[84]
Hemp fiber	158.7	31.1	5.10	5.92	5.61	20	1.056	0.7-mm diameter	V	[84]
Hemp fiber	115.0	40.5	2.84	3.10	3.12	20	0.993	0.8-mm diameter	V	[84]
Hemp fiber	92.0	25.6	3.59	4.03	3.95	20	1.021	0.9-mm diameter	V	[84]
Bamboo fiber	671.9	278.5	2.41	2.43	2.65	20	0.915	20-mm gage length	V	[85]
Bamboo fiber	641.6	191.3	3.35	3.35	3.69	20	0.908	30-mm gage length	V	[85]
Bamboo fiber	581.1	209.4	2.77	2.99	3.05	20	0.980	40-mm gage length	V	[85]
Bamboo fiber	581.1	101.7	5.71	6.06	6.29	20	0.964	50-mm gage length	V	[85]

* This unpublished data was provided by K. Naito. D/V stands for data type of D = digitized and V = Values from the literature. Ref = reference number.

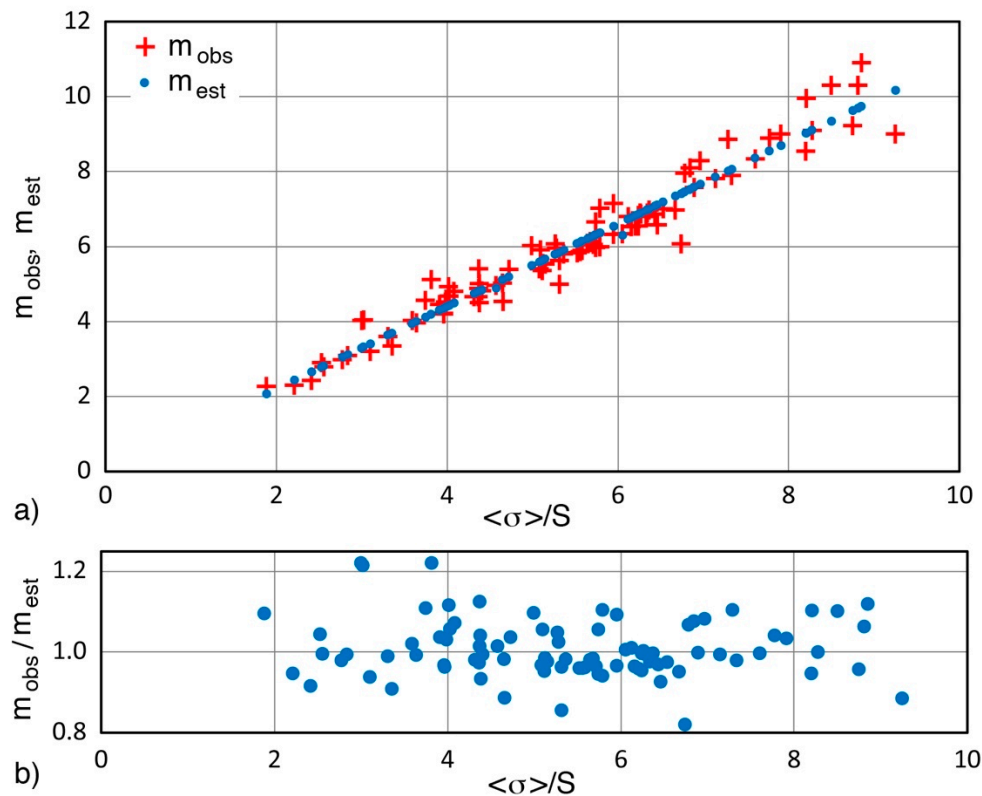


Figure 7. (a) Plots of m_{obs} (red + symbol) and m_{est} (blue dot) vs. $\langle\sigma\rangle/S$ for fiber data. (b) Plot of m_{obs}/m_{est} (blue dot) vs. $\langle\sigma\rangle/S$ for the same.

One of the reasons that fiber m values are low is the variation of fiber diameter along the length. Some studies have considered diametral effects [86,87], but it is difficult to separate them in general. Due to the high strength levels that fibers achieve, extremely small flaws can induce fracture [88,89]. That is another source of low m values, making Weibull analysis an essential part of fiber studies.

4.5. Composites

Table 6 lists the strength and Weibull modulus data of composite materials. For these datasets, the average of m_{obs}/m_{est} is 0.992, and the standard deviation is 0.088. The average m_{obs}/m_{est} value is 2% lower than that of the entire data, while the general trends seen in Figure 8 appear to skew slightly to lower m_{obs} as the m values increase. However, high m_{obs}/m_{est} values are mostly populated at low m values in Figure 8b. The m value of composites reached 44, exceeded only by ductile metals. Many Weibull studies were conducted earlier, but typically no values of $\langle\sigma\rangle$ and S were included. Two articles are useful in finding Weibull modulus values for many composites not included here [27,90]. Another article to be noted is [91], as it included many lay-ups and tested at different loading rates. However, the sample counts were three for each condition, so it is hardly worth calling it a “statistical” study. However, no similar tests appear to exist, and it may serve as a preliminary guide. In regard to small sample counts, four datasets with $N = 5$ are included in Table 6 for glass fiber composites. They used samples of large diameter (12 to 18 mm), and the tests followed an industrial guideline [17] for concrete-reinforcing bars. Since the m values were from 20 to 40, the sample count of five or more was deemed adequate for quality control purposes.

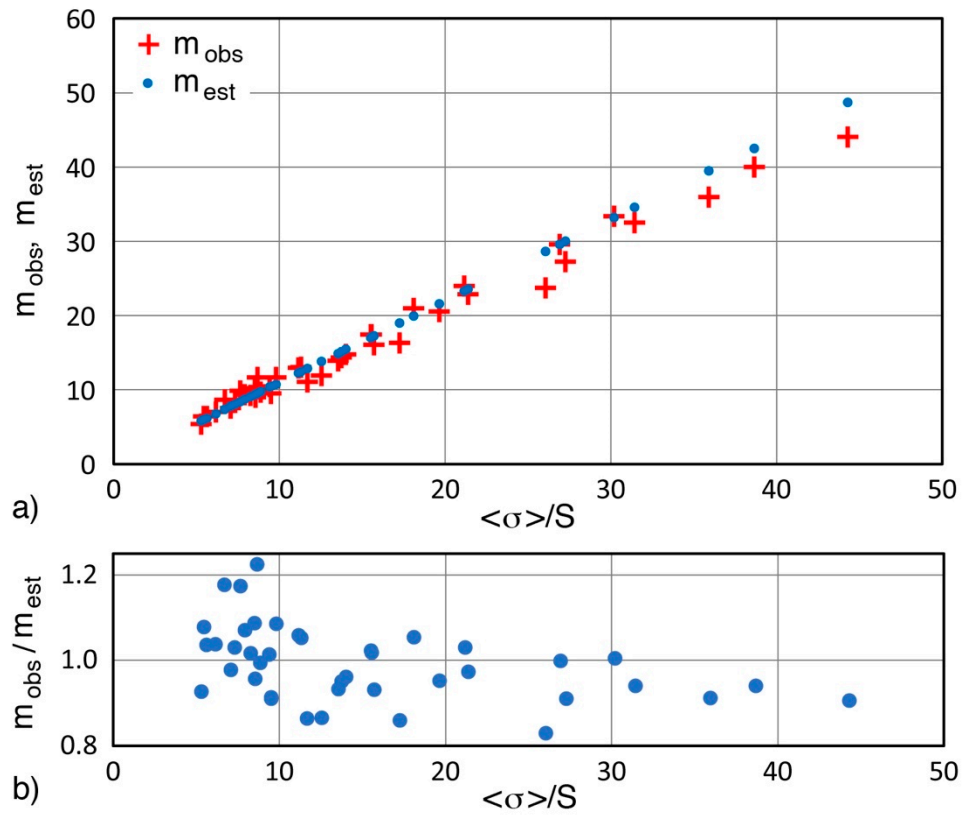


Figure 8. (a) Plots of m_{obs} (red + symbol) and m_{est} (blue dot) vs. $\langle\sigma\rangle/S$ for composite data. (b) Plot of m_{obs}/m_{est} (blue dot) vs. $\langle\sigma\rangle/S$ for the same.

Table 6. Listing of data for composites.

Composites	$\langle\sigma\rangle$	S	$\langle\sigma\rangle/SD$	m_{obs}	m_{est}	N	m_{obs}/m_{est}	Note	D/V	Ref
CFRP unidirectional	2504.0	82.9	30.22	33.41	33.25	35	1.005	Fiber fraction 0.68	V	[92]
CFRP unidirectional	2751.0	62.1	44.30	44.10	48.73	35	0.905	Fiber fraction unknown	V	[92]
CFRP unidirectional	2237.4	83.1	26.92	29.58	29.62	35	0.999	Fiber fraction 0.62	V	[92]
CFRP unidirectional	2497.6	223.9	11.15	12.98	12.27	105	1.058	Combined	V	[92]
CFRP unidirectional	2718.0	127.0	21.40	22.90	23.54	20	0.973	IM600 fiber	V	[93]
CFRP unidirectional	1638.0	119.0	13.76	14.40	15.14	20	0.951	K13D fiber	V	[93]
CFRP unidirectional	1337.0	68.0	19.66	20.60	21.63	20	0.952	Combined	V	[93]
C/glass hybrid rod	1423.0	54.6	26.06	23.77	28.67	10	0.829	T700SC/E-glass K241P	D	[94]
C/glass hybrid rod	1803.0	66.1	27.28	27.29	30.00	10	0.910	T700SC/E-glass K242P	D	[94]
C/glass hybrid rod	1837.0	58.4	31.46	32.50	34.60	10	0.939	T700SC/E-glass K243P	D	[94]
CFRP unidirectional	1815.0	117.0	15.51	17.44	17.06	13	1.022	T700 fiber	D	[95]
CFRP unidirectional	2209.0	157.4	14.03	14.83	15.44	13	0.961	TC35 fiber	D	[96]
CFRP unidirectional	3156.0	270.0	11.69	11.11	12.86	12	0.864	T700-T600 fiber	D	[96]
CFRP unidirectional	1695.0	107.8	15.72	16.11	17.29	23	0.932	Ring-NOL test	D	[97]
CFRP unidirectional	1660.0		6.17	7.04	6.79	78	1.037	PA6 resin	V	[97]
CFRP unidirectional	2428.0		5.46	6.48	6.01	52	1.078	Epoxy resin	V	[97]
CFRP unidirectional	496.0	31.9	15.57	17.44	17.12	19	1.018	Fiber fraction 0.28	V	[98]
Woven CFRP	246.0		7.94	9.34	8.73	15	1.070	PA6 resin	V	[99]
Woven CFRP	316.4		9.80	11.70	10.78	15	1.085	Dispersion treated	V	[99]
GFRP unidirectional	528.7	39.0	13.56	13.90	14.91	10	0.932	Strain rate 0.0017/s	D	[100]
GFRP unidirectional	541.6	56.9	9.52	9.53	10.47	10	0.910	Strain rate 25/s	D	[100]
GFRP unidirectional	585.0	33.9	17.26	16.30	18.98	9	0.859	Strain rate 50/s	D	[100]
GFRP unidirectional	633.7	50.5	12.55	11.95	13.80	9	0.866	Strain rate 100/s	D	[100]
GFRP unidirectional	740.6	78.0	9.49	9.54	10.44	9	0.913	Strain rate 200/s	D	[100]
GFRP reinforcing bar	1818.0	47.0	38.68	40.00	42.55	5	0.940	14-mm diameter	V	[101]
GFRP reinforcing bar	1653.0	46.0	35.93	36.00	39.53	5	0.911	18-mm diameter	V	[101]
GFRP reinforcing bar	2010.0	111.0	18.11	21.00	19.92	5	1.054	12-mm diameter	V	[101]
GFRP reinforcing bar	1927.0	91.0	21.18	24.00	23.29	5	1.030	16-mm diameter	V	[101]
GFRP short fiber	257.0	31.1	8.26	9.24	9.09	20	1.016	Sheet molding compound	D	[102]
ZrO ₂ -SiO ₂ composite	149.4	20.4	7.32	8.30	8.06	30	1.030	60% particulate	V	[103]
ZrO ₂ -SiO ₂ composite	154.0	13.6	11.32	13.10	12.46	30	1.052	60% particulate	V	[103]
ZrO ₂ -SiO ₂ composite	135.7	15.3	8.87	9.70	9.76	30	0.994	60% particulate	V	[103]
ZrO ₂ -SiO ₂ composite	140.7	19.9	7.07	7.60	7.78	30	0.977	60% particulate	V	[103]
Zirconia 0%-TiO ₂	815.4	145.1	5.62	6.40	6.18	30	1.035	with 3% Y ₂ O ₃	V	[104]
Zirconia 0%-TiO ₂	763.6	144.2	5.30	5.40	5.82	30	0.927	with 3% Y ₂ O ₃	V	[104]

Table 6. Cont.

Composites	$\langle\sigma\rangle$	S	$\langle\sigma\rangle/SD$	m_{obs}	m_{est}	N	m_{obs}/m_{est}	Note	D/V	Ref
Zirconia 10%–TiO ₂	455.7	48.4	9.42	10.50	10.36	30	1.014	with 2.7% Y ₂ O ₃	V	[104]
Zirconia 10%–TiO ₂	439.4	65.4	6.72	8.70	7.39	30	1.177	with 2.7% Y ₂ O ₃	V	[104]
Zirconia 30%–TiO ₂	336.0	38.7	8.68	11.70	9.55	30	1.225	with 2.1% Y ₂ O ₃	V	[104]
Zirconia 30%–TiO ₂	334.2	43.6	7.67	9.90	8.43	30	1.174	with 2.1% Y ₂ O ₃	V	[104]
SiC/SiC composite	597.0	70.0	8.53	10.20	9.38	34	1.087	Flexure strength	D	[105]
C/SiC composite	101.8	11.9	8.56	9.00	9.42	11	0.956	Tensile strength	D	[106]

D/V stands for data type of D = digitized and V = Values from the literature. Ref = reference number. CFRP and GFRP stand for carbon fiber and glass fiber reinforced plastics.

4.6. Summary

It is shown in this section that Equation (14) provides the best correlation between the observed Weibull modulus and estimated values from the average and standard deviation (or the coefficient of variation) of experimentally determined strength datasets; that is, $m = 1.1 <\sigma>/S = 1.1/CV$ (modified Robinson relation). This conclusion is based on a comparison of these values from more than 260 datasets. Estimated m values matched to normally calculated m_{obs} values on average within 1%, and each pair of m values was within $\pm 20\%$ except for 11 cases.

5. Discussion

5.1. Estimation of m from Standard Deviation or from Coefficient of Variation

Using the modified Robinson relation, it is now possible to estimate the Weibull modulus when only the average and standard deviation of a strength dataset are known. Two interlaboratory studies on mechanical testing standards that were cited earlier contain base data for many materials [24,25]. These studies aimed to define the reproducibility, R , of mechanical tests conducted at different laboratories. The reproducibility includes interlaboratory deviations of strength calibration, deviations due to sample chemistry and process variables, test conditions, etc., since the main aim of these studies was to establish the accuracy of mechanical test results. The ASTM study [24] separately reported the standard deviation for within-laboratory precision, s_r , that for between-laboratory precision, s_R , and R . ASTM standard E8 provided these parameters for six alloys (two Al alloys, three steel alloys, and one Ni alloy) [107]. This ASTM E8 shows that the reproducibility R is three to six times larger than the standard deviation of a single series of tests at one location, s_r , while National Physical Laboratory (NPL) report [108] put the factor at four on average. Thus, the s_R values can be used for estimating m values when samples come from a single set. When many sets of samples from multiple sources are tested at different sites, R values are appropriate. These two reports provided the average tensile strength and standard deviation for 20 different alloys (six for Al alloys, 12 for steel alloys, and three for Ni alloys). The m_{est} values from the ASTM E8 [107] and NPL report [108] are shown in Table 7. While the m_{est} values for Al (45 to 82) and A105 steel (75) are comparable to the previously known values in Table 3, the m_{est} values for 316 and 51410 steels and Inconel[®] 600 are higher (91, 174, and 151). From NPL collected data, the m_{est} of Al alloys are again comparable at 47 to 122, while steel and Ni alloy resulted in m_{est} values of 44 to 169. Again, the m values reported fit the range found in Table 3, where the m_{est} values of structural steels were from 44 to 110, while those of stainless steels and Ni alloys were from 37 to 175.

Table 7. Listing of data for estimated m values using S or coefficient of variation (CV) and for observed m.

Materials	$\langle\sigma\rangle$	S	CV	M_{obs}	M_{est}	N	Note	Ref
Aluminum EC-H19	176.90	4.3			45.25	NA	7-1	[107]
Al 2024-T351	491.30	6.6			81.88	NA		[107]
A105 steel	596.90	8.7			75.47	NA	ASTM grade	[107]
316 stainless steel	694.60	8.4			90.96	NA		[107]
Inconel® 600 Ni	685.90	5.0			150.90	NA		[107]
51410 steel	1253.00	7.9			174.47	NA	410 martensitic SS	[107]
Al 5754	212.30		0.0235		46.81	NA	7-2	[108]
Al 5182-O	275.20		0.012		91.67	NA		[108]
Al 6016-T6	228.30		0.009		122.22	NA		[108]
DX56 steel sheet	301.10		0.025		44.00	NA		[108]
Low C HR3 steel	335.20		0.025		44.00	NA		[108]
ZSt180 steel sheet	315.30		0.021		52.38	NA		[108]
Fe510C steel	552.40		0.01		110.00	NA		[108]
S355 steel plate	564.90		0.012		91.67	NA		[108]
316L stainless steel	568.70		0.0295		37.29	NA		[108]
X2CrNi18-10 SS	594.00		0.015		73.33	NA	304 SS	[108]
X2CrNiMo18-10 SS	622.50		0.015		73.33	NA	316 SS	[108]
30NiCrMo16 SS	1153.00		0.007		157.14	NA		[108]
Nimonic® 75	754.20		0.0065		169.23	NA		[108]
18Ni Maraging steel	1147.30	11.12		99.00	113.49	9	Laser sintered	[51]
18Ni Maraging steel	1290.00	56.15			25.27	3	Laser sintered	[51]
18Ni Maraging steel	1324.00	51			28.56	3	Laser sintered	[51]
18Ni Maraging steel	1142.70	18.6			67.58	3	Laser sintered	[51]
18Ni Maraging steel	1142.90	25.8			48.73	3	Laser sintered	[51]
18Ni Maraging steel	1156.20	7.1			179.13	3	Laser sintered	[51]
Dual-phase steel	987.00	26			41.76	5	Strain rate 948/s	[109]
Dual-phase steel	917.00	21			48.03	5	1740/s	[109]
Dual-phase steel	920.00	22			46.00	5	2906/s	[109]
Dual-phase steel	562.00	17			36.36	5	0.001/s	[109]
Dual-phase steel	828.00	22			41.40	5	1134/s	[109]
Dual-phase steel	812.00	46			19.42	5	1882/s	[109]
Dual-phase steel	823.00	25			36.21	5	3158/s	[109]
316LVM SS	1024.00	12			93.87	NA	As received 7-3	[110]
316LVM SS	1795.00	21			94.02	NA	Extrusion 184%	[110]
Ti-6Al-4V	917.70	29.8			33.87	48		[111]

Table 7. Cont.

Materials	$\langle\sigma\rangle$	S	CV	M_{obs}	M_{est}	N	Note	Ref
Copper	150.00	27			6.11	24	As received	[112]
Copper	413.00	18			25.24	24	Cold rolled	[112]
Cu-44Ni alloy	300.00	28			11.79	24	As received	[112]
Cu-44Ni alloy	722.00	50			15.88	24	Cold rolled	[112]
Al 2030	490.00	1.46			369.18	15	Laboratory practice	[113]
Al 2030	487.00	3.64			147.17	15	Automated-industrial	[113]
Dental wires	1845.80	142.3			14.27	NA	316 SS cold drawn 7-4	[114]
Dental wires	874.10	275.9			3.48	NA	Ti-Mo alloy	[114]
Dental wires	1449.80	156.6			10.18	NA	Co-Cr alloy	[114]
AerMet100 [®] steel	1966.60	50.9			42.50	5	Tensile strength	[115]
AerMet100 [®] steel	142.50	37.5		2.96	4.17	6	K_{Ic}	[115]
AerMet100 [®] steel	101.18	52.75			2.11	6	J_{Ic}	[115]
Brittle solids				4.00		NA	theory	[116]
CNT fibers	1241.00	261			5.23	10	reference	[117]
CNT fibers	1375.00	187			8.09	10	coating 1	[117]
CNT fibers	972.00	160			6.68	10	coating 2	[117]
CNT fibers	1240.00	246			5.54	10	coating 3	[117]
CNT fibers	1073.00	162			7.29	10	reference	[117]
CNT fibers	1336.00	119			12.35	10	coating 1	[117]
CNT fibers	1455.00	173			9.25	10	coating 2	[117]
CNT fibers	1214.00	134			9.97	10	coating 3	[117]
CNT fibers	714.00	26			30.21	10	reference	[117]
CNT fibers	616.00	86			7.88	10	coating 1	[117]
CNT fibers	700.00	48			16.04	10	coating 2	[117]
CNT fibers	826.00	80			11.36	10	coating 3	[117]
CNT				1.70		26	Multi wall	[118]
CNT				2.40		NA	Multi wall 7-5	[118]
CNT bundles				2.70		NA		[118]
CNT fibers	300.00			4.30		60	Low strain rate	[119]
CNT fibers	650.00			6.80		85	High strain rate	[119]
CNT	31,200	11,839		2.23	2.90	19	Single CNT	[120]
CNT				2.48		9	Multiwall CNT	[121]
Mid-Hudson Bridge	1609.07	51.66		32.10	34.26	>10	Location: 1N-2N	[43]
Mid-Hudson Bridge	1608.26	64.49			27.43	>10	42N 43N	[43]
Mid-Hudson Bridge	1609.18	67.67			26.16	>10	89N 90N	[43]
Mid-Hudson Bridge	1613.44	53.71			33.04	>10	133 134	[43]
Mid-Hudson Bridge	1634.38	66.98			26.84	>10	3s4s	[43]

Table 7. Cont.

Materials	$\langle\sigma\rangle$	S	CV	M _{Obs}	M _{Est}	N	Note	Ref
Mid-Hudson Bridge	1635.55	65.27			27.56	>10	61-62	[43]
Mid-Hudson Bridge	1637.76	77.14			23.35	>10	90-91s	[43]
Mid-Hudson Bridge	1599.07	59.80			29.42	>10	136-137s	[43]
Bridge W	1695.00		0.026		42.31	17	Corrosion Stage 2	[122]
Bridge W	1695.00		0.026		42.31	17	Stage 3	[122]
Bridge W	1661.10		0.038		28.95	35	Stage 4	[122]
Bridge W	1508.55		0.128		8.59	11	Stage 4 + Cr	[122]
Bridge X	1647.06		0.018		61.11	30	Stage 2	[122]
Bridge X	1625.52		0.024		45.83	18	Stage 3	[122]
Bridge X	1592.38		0.038		28.95	10	Stage 4	[122]
Bridge X	1381.94		0.131		8.40	15	Stage 4 + Cracks	[122]
Bridge Z	1644.00		0.021		52.38	20	Stage 1	[122]
Bridge Z	1620.98		0.029		37.93	29	Stage 2	[122]
Bridge Z	1553.58		0.039		28.21	22	Stage 3	[122]
Bridge Z	1551.94		0.041		26.83	33	Stage 4	[122]
Bridge Z	1144.22		0.263		4.18	6	Stage 4 + Cracks	[122]
Al-Cu casting				4		36		[123]
Al-Cu casting				4		36		[123]
White cast iron				2		26		[123]
White cast iron				2		21		[123]
Gray cast iron				6		17		[123]
Al casting A357-T6	357			47.5		354		[124]
Al casting A357-T6	361			30.6		388		[124]
Al 7Si casting				10.79		45		[125]
Al 7Si casting				19.71		40		[125]
Al 7Si casting				37.74		36		[125]
Al 7Si casting				20.87		80		[125]
Al 7Si casting				2.5		30		[126]
Al 7Si casting				6.4		30		[126]
Al 7Si casting				13.7		30	Bimodal, low	[126]
Al 7Si casting				20		30	Bimodal, high	[126]
AM60B Mg casting				7.69		18	As cast	[127]
AM60B Mg casting				13.52		18	T6 heat treatment	[127]

Ref: reference number; Note 7-1: NA = not available, but expected to be above 30 for [107]; Note 7-2: NA= not available, but expected to be above 50 for [108]; Note 7-3: NA = not available for [110]; Note 7-4: NA = not available for [114]; Note 7-5: NA = not available for [118]. CNT = carbon nanotubes.

Two groups of steel in Table 3 have lower m values of 15 to 29, but these were sintered materials that were expected to contain numerous voids. The following six rows in Table 7 are the data from laser-sintered maraging steel [51]. The first row was listed in Table 3 as it included nine strength values. Its m_{obs} value was calculated as 99.2, which agreed reasonably with the m_{est} of 113.5 with the modified Robinson relation. Other m_{est} values given here were between 25–179, reflecting the variability of the selective laser melting process used. However, the last row with an m value of 179 is clearly out of the range. The estimated m values should lead to a better selection of process parameters, since normally sintered medium carbon steel showed m values within the range of 15 to 27 [52], as shown in Table 3. The seven datasets that follow are from dual-phase steel with ferrite and martensite phases [109]. The carbon level is low (0.11–0.12%), producing a uniform strain of more than 10%. Estimated m values ranged from about 20 to 113, and most were in the 30 to 50 range. The case of the highest m value was for quasi-static loading, and the yield strength also showed a low scatter, making the high m value plausible (one dataset was not included since only a one-digit S value was given).

The next 15 rows in Table 7 covered various alloys with a wide range of m values. Most of them are roughly comparable to the similar alloys given in Table 3. Ti–6Al–4V [111] is the only Ti alloy in this work, and is similar to 316L stainless steel in the NPL study above [108]. Copper and Cu–Ni [112] showed comparable m values (except as received Cu) to the reported m values of 12 to 16 for pure Cu in [48] in Table 3. The Al 2030 results showed high m values, but also indicated sensitivity to test conditions. As noted earlier, more elaborate tests are needed to verify m values over 100. The last three rows in this group are for AerMet100® steel (Carpenter Tech. Corp, Philadelphia, PA, USA), which has high strength and fracture toughness [115]. It is of composition, 0.23C–13.4Co–11.1Ni–3.1Cr–1.2Mo, and is used in age-hardened martensitic state (or maraging steel). The tensile strength data gives an m value of 43, which can be expected for a low C, high-strength Co–Ni steel. While the fracture toughness (K_{IC} or J_{IC}) levels are high, the estimated m values are low (2 to 4) using an N of 5 or 6. The Weibull plot of the K_{IC} data also showed $m = 3$. This level of m is consistent with the m values of 2 to 10 that are generally obtained in brittle fracture as reported by Wallin et al. [32,116], who theoretically predicted $m = 4$ for K_{IC} of generic brittle solids. This should make designers cautious, despite its high fracture toughness.

The next group of 12 datasets is for fibers made from carbon nanotubes (CNT) [117]. Only averaged strength data is available, giving estimated m values between 5–30. A few of them were higher than any m value for the fibers in Table 5, while the majority fitted to the range of regular fibers. A previous work on CNT bundles showed m values of 1.7 to 2.7 [118] and 4.3 to 6.8 [119], while a single CNT has an m value of about 3 [120,121]. When the strength data of a single CNT in [120] was analyzed, $m_{\text{obs}} = 2.3$ and m_{est} of 2.9 were obtained, implying that the present method works at the nanoscale as well. However, deviation is higher, as the CNT has the tensile strength of 11 to 63 GPa.

In two engineering studies of suspension cable wires, the average and standard deviation of strength data of suspension cable wires were reported. One was from the Mid-Hudson Bridge [44], containing a dataset with $m_{\text{obs}} = 32.07$. This was included in Table 2. Remaining datasets of only the average plus standard deviation are listed in Table 7. These give m values of 23 to 35, matching the m_{obs} value for one of the samples. These represent Stage 4 corrosion according to [23]. Visually, these wires were judged to be Stage 2 to 3. Another report gave results from three suspension bridges: X, W, and Z [122]. This study included wires of various corrosion stages, 1 to 4 plus cracked. Roughly half of the wires showed m values that were in agreement with visual inspection, but others showed more damages according to the m values observed. Since tensile testing is part of the standard procedures in maintenance inspection, the present simple m estimation method provides a quantitative tool to evaluate the wire inspection results.

In estimating m with the data on standard deviation or CV values, it is necessary to use caution, since some sources apparently discard low strength values in the tail part of distribution. This is especially true for the data without giving a sample count, N . Some testers used N values of 5 to 6 for CV values and need added scrutiny, as results can be unreliable. When this critical information is

unavailable, it is best to avoid them. For example, Salem [47] collected 19 CV values on commercial ceramics with low K_{Ic} values in the range of 2.2 to 6.1 MPa \sqrt{m} . Corresponding CV values were 0.008 to 0.104, yielding m values of 10.8 to 134 with an average of 31.7. Nine of 19 exceeded $m = 20$. These results certainly contradict the above conclusion of Wallin [116] and the results in Table 4. Salem concluded that no relationship exists between fracture toughness and CV, but it is plausible that the CV data he collected was unrepresentative of real ceramics behavior. Another issue in S or CV values is the rounding of the data. Some reports provided only single digit values, and such data cannot be used unless rough estimates are acceptable.

The values of m_{est} are mostly within $\pm 20\%$ of m_{obs} from a Weibull plot of the base strength data. This $\pm 20\%$ limit is based on 71 datasets in the present study, which started from a listing of strength values, and the values of m_{obs}/m_{est} ratios were calculated. The average was 0.98 ($S = 0.088$), and the m_{obs}/m_{est} ratio ranged from 0.79 to 1.19. This limit can be used to judge the m and CV values from the literature. When these two values are off from the modified Robinson relation by more than 20%, one or the other value is likely to be in error. The most common source is the trimming of outliers to make the CV smaller. In the above direct comparison of m_{obs} and m_{est} from the same strength data, two cases were at 0.79. These were both from historic iron data. When the two old cases (listed in Table 2) are censored, the range is reduced to 0.83 to 1.15, and the $\pm 20\%$ limit is conservative.

In many brittle solids, more than one type of flaw may control the fracture, leading to a bimodal Weibull distribution. An example is given in ASTM C1239 [128]. A bimodal Weibull distribution is shown in Figure 2 and in the data in Table 5 in the C1239 standard with a sample count of 79. It follows the slope of $m = 6.79$ on the low side, and $m = 21.0$ above a fracture strength of 620 MPa. When the data is replotted and a single m value is calculated, one obtains $m_{obs} = 9.98$, while the average strength was 659.23 MPa and standard deviation was 59.56 MPa, yielding $m_{est} = 12.18$. Thus, $m_{obs}/m_{est} = 0.825$, which fits with the normal pattern of m estimation. This shows that the present method can be used for the bimodal cases, averaging the two slope regions. However, an arbitrary cut-off of the original data on the low end will raise the m value toward the high slope. A unimodal example in ASTM C1239 [128] has $m_{obs} = 6.38$. Using the data given in Table 4 of C1239, m_{obs} , $\langle\sigma\rangle$, and S were calculated using the methods of this study, and resulted in $m_{obs} = 6.52$ and $m_{est} = 6.23$. These three m values match well, showing that a valid S (or CV) value will lead to a satisfactory estimate of m .

Cast iron has long been known for its brittleness, but it has been used widely despite its drawbacks. Weibull moduli of white and gray cast iron are indeed low at 2 and 6 [123]. Other cast alloys showed varied behavior. For example, an Al–Cu alloy casting [123] had $m = 4$, while Al–Si casting alloys had m_{obs} of 60 to 116 [54] (see Table 3). Two extensive tests of A357 Al castings confirmed high m_{obs} values for high-quality Al castings. Using 354 and 388 samples, m_{obs} values of 47.5 and 30.6 were obtained [124]. For Al–7Si and Mg AM60 castings, three studies reported m_{obs} values from 2.5 to 38 [125–127]. It is clear that cast alloys need to be treated separately from wrought alloys and between castings made from different processes.

5.2. Industrial Strength Data

When one examines strength data from metal industry, the deviation of data is often given in terms of standard deviation. While the normal distribution can represent the data well, it is often useful to describe the data with Weibull distribution, as it will allow advanced data analyses, such as failure and lifetime prediction. A short list of large-scale studies of steel strength are collected and summarized in this section, providing representative m values estimated, as listed in Table 8. One notable feature is that the sample counts are high, making the outcome more reliable. Two related works are also added.

Table 8. Listing of large-scale data for estimated m values using S or CV and for observed m.

Materials	$\langle\sigma\rangle$	S	CV	M_{Obs}	M_{est}	N	Note	Ref
S355MC steel	497.44	11.31			48.38	703	Hot-rolled sheet	[129]
ABS A steel	408.79		0.044		25.00	33	1948 tests	[130]
ABS B steel	420.72		0.091		12.09	79	1948 tests	[130]
ABS C steel	415.54		0.051		21.57	13	1948 tests	[130]
ABS B steel	431.55		0.044		25.00	39	Before 1984	[130]
ABS C steel	436.03		0.047		23.40	36	Before 1984	[130]
ASTM A7 steel	432.03		0.0226		48.67	120	Before 1984	[130]
ASTM A7 steel	443.68		0.0341		32.26	58	Before 1984	[130]
ASTM A7 steel	418.23		0.0241		45.64	54	Before 1984	[130]
ASTM A7 steel	416.65		0.0719		15.30	22	Before 1984	[130]
Q235 steel	456.87	21.73			23.13	3924	2.5 to 16-mm thick plates	[131]
Q235 steel	446.45	20.02			24.53	7371	16 to 40 mm	[131]
Q235 steel	442.33	22.26			21.86	1861	40 to 60 mm	[131]
Q235 steel	437.20	21.61			22.25	718	60 to 100 mm	[131]
Q235 steel	431.76	19.3			24.61	170	100 to 150 mm	[131]
Q235 steel	448.16	21.75			22.67	14,044	Total of above	[131]
Q345 steel	553.08	28.1			21.65	2632	2.5 to 16-mm thick plates	[131]
Q345 steel	539.20	31.05			19.10	2230	16 to 40 mm	[131]
Q345 steel	527.15	27.32			21.22	646	40 to 60 mm	[131]
Q345 steel	527.83	28.2			20.59	396	60 to 100 mm	[121]
Q345 steel	513.94	27.38			20.65	36	100 to 150 mm	[121]
Q345 steel	543.13	30.45			19.62	5940	Total of above	[131]
S235JR steel	465.90	51.6			9.93	120	ASTM A283C #	[132]
S335J2+N steel	569.70	29.1			21.54	31	ASTM A527-50 #	[132]
S550C steel	678.10	37.3			20.00	23	ASTM X80XLK #	[132]
S235UNI steel	316.16	24.46			14.22	689	Hot rolled	[133]
S275SHS steel	377.33	21.09			19.68	290	Hot rolled	[133]
S275BS steel	310.95	14.34			23.85	4095	Hot rolled	[133]
S355BS steel	402.02	16.13			27.42	1914	Hot rolled	[133]
S460BS steel	474.64	20.24			25.80	672	Hot rolled	[133]
CSA G40.20 450W	450 *		0.035		31.43	4942	W shapes	[134]
CSA G40.20 450W	450 *		0.04		27.50	10,794	W shapes	[134]
CSA G40.20 450W	450 *		0.03		36.67	2873	W shapes	[134]
CSA G40.20 450W	450 *		0.047		23.40	987	W shapes	[134]

Table 8. Cont.

Materials	< σ >	S	CV	M _{Obs}	M _{est}	N	Note	Ref
CSA G40.20 450W	450 *		0.032		34.38	407	W shapes	[134]
CSA G40.20 450W	450 *		0.04		27.50	10,652	W shapes	[134]
CSA G40.21 300W	300 *		0.045		24.44	973	Class C/H bars	[134]
CSA G40.21 300W	300 *		0.062		17.74	730	Class C/H bars	[134]
CSA G40.21 350W	350 *		0.035		31.43	73	Class C/H bars	[134]
CSA G40.21 350W	350 *		0.054		20.37	188	Class C/H bars	[134]
CSA G40.21 350W	350 *		0.056		19.64	815	Class C/H bars	[134]
CSA G40.21 300W	300 *		0.051		21.57	407	Class C/H bars	[134]
CSA G40.21 300W	300 *		0.058		18.97	374	Class C/H bars	[134]
CSA G40.21 350W	350 *		0.049		22.45	64	Class C/H bars	[134]
CSA G40.21 350W	350 *		0.052		21.15	174	Class C/H bars	[134]
S275 steel	451.00	21.7			22.86	1547	Reinforcing bars	[135]
S380 steel	695.20	42.52			17.98	388	Reinforcing bars	[135]
ASTM A615-60 steel	676.00	21.93			33.91	130	Reinforcing bars	[136]
High C steel wire	1653	19.2			94.7	38,470	Suspension cable	[15]
High C steel wire	1660	17.1			97.1	45	Suspension cable	[15]
				Median m	m range			
Cast iron pipes				9	1 to 29	512	Undamaged zone	[137]
Cast iron pipes				7	1 to 23	650	Light damage	[137]
Cast iron pipes				6	1 to 23	542	Moderate damage	[137]
Cast iron pipes				2	1 to 14	542	Heavy damage	[137]
				Average m	m range			
Graphite				9.74	6.8 to 13.4	2000	Nuclear grade	[138]

Equivalent steel grade; * Nominal tensile strength for CSA G40 grades. CSA stands for Canadian Standards Association. ABS stands for American Bureau of Shipping. Ref: reference number.

a. Hot-rolled steel [129]

Evaluating the strength of 703 coils of this high-strength low-alloy (HSLA) steel, S355MC, the average and S value provided an m_{est} of 48.4. See Table 8.

b. Shipbuilding steels [130]

The published data of nine groups of shipbuilding steels was tabulated, from which m values were estimated. Steels are types A, B, and C of the American Bureau of Shipping (ABS) and ASTM A7. These grades were superseded by newer grades in the 1960s, but all were weldable low-carbon steels. The m_{est} values were from 12 to 48.7.

c. Chinese HSLA steels [131]

Q235 and Q335 (corresponding to S235 and S355) steels from four steel mills were tested. Data for a total of 20,086 plates was listed, and their m_{est} values for six groups each are given in Table 8. The results are tightly distributed between 19–24.6. These steels were made for the penstocks of hydropower stations. The weighted m_{est} average was 22.3.

d. Plain carbon and HSLA steels, S235, S355, and S550 [132]

Standard grade steels had m_{est} ranging from 10 to 22. The high S (low m_{est}) value for S235 steel was attributed to the mill practice of mixing subgrade steels, but the tests included four different structural shapes, and different processing may also be a factor. In addition, the minimum strength value was 50 MPa below the required strength for equivalent ASTM A283 steel.

e. Hot-rolled steels [133]

This study provided strength data for various shapes, and those for hot-rolled plates are shown here. Samples counts are large (290 to 4095) and yielded m_{est} values of 14 to 27 for five grades of steel.

f. Steel shapes [134]

This work summarized a collection of Canadian steel data of 34,453 samples. The strength values were mostly collected from mill certificates. For steels of 300, 350, and 450 MPa (nominal) tensile strength, m values were found to range from 18 to 37. The weighted m average was 28.2. The Canadian and Chinese studies [131,134] used large sample counts and produced the most consistent and representative m values of contemporary HSLA steels, that is, m_{est} is 22.3 to 28.2. These values are approximately one-half of the lower limit of m_{obs} observed in the laboratory studies as discussed in Sections 4.2 and 5.1. As noted previously, this reduction in m (or increase in CV) is caused by additional deviation due to chemistry variations, process differences between steel mills, and test procedures, among others. In terms of the parameters used in the ASTM E28 study [24], it is the R parameter that governs the deviation for large-scale studies. Thus, the observed reduction in m_{est} is expected.

g. Reinforcing bars [135,136]

Two studies examined steel-reinforcing bars and showed m values of 18 to 34.

h. High strength suspension cable wires [15]

Two datasets of high C steel strength, one from the Bisan Seto Bridge in Japan with $N = 38,470$ (completed in 1988), showed m values of 94 to 97, with the strength levels reaching 1.65–1.66 GPa.

i. Cast iron pipes [137]

In spite of its known lack of ductility, cast iron pipes have been used for water distribution systems at many cities. This study reported results of a systematic examination of buried cast iron pipes in and around London, UK. Samples were excavated from 119 locations that were known to be in four different stages of deterioration: undamaged, lightly damaged, moderately damaged, and heavily damaged. The number of pipe samples, which were 0.5 to 1 m in length, was 34, 43, 36, and 36 at each stage, and about 15 samples were tested in flexure for each pipe sample. Nearly 1800 flexure strength tests were conducted. The results were analyzed, and most of the Weibull modulus values were found to be below 10, as indicated in Table 8. The damage stages and median m_{obs} values appear to be correlated, but the m_{obs} value is so low, even in the sound state. Thus, improved nondestructive testing methods may be more beneficial for identifying the damage states of buried pipes [139].

j. Graphite [138]

A large-scale testing of nuclear-grade graphite examined the Weibull moduli of 2000 samples and listed the results in eight groups. A summary is given in Table 8, showing low m_{obs} values of 6.8 to 13.4. These are lower than those for NBG18 in Table 4. In these studies, sample counts were within a factor of 2.3, and quality differences may be the cause.

k. Large-scale testing

In most of the large testing projects reviewed here, Weibull analysis was not included. The simple estimation method improved in this study can easily add Weibull modulus data to elaborate data collection and analysis conducted in metal and construction industries and elsewhere. The m values will be beneficial in subsequent analyses, such as those conducted in the structural health monitoring of structures [140].

6. Conclusions

1. Methods of estimating Weibull modulus (m) of an experimentally obtained dataset were examined. These utilized the average ($\langle\sigma\rangle$) and standard deviation (S) (or coefficient of variation, CV) based on the normal distribution. Several approximate relationships have been proposed starting from Robinson [11], but all of them deviate from the exact expression given with the gamma function.
2. The exact expression can be represented by $m = 1.271 \langle\sigma\rangle/S = 1.271/CV$ with $R^2 = 0.9999$. Robinson used 1.20 as the constant [11].
3. In order to obtain m values that fit with the actually observed material strength datasets, a reduction of the constant from 1.271 to 1.10 is found to be optimal. This produces the modified Robinson relation of $m = 1.10 \langle\sigma\rangle/S = 1.10/CV$, which can estimate m values that are in good agreement with the m values obtained from Weibull analyses. This agreement was verified by over 260 datasets of the strength of metals, ceramics, fibers, and composite materials, with most of the data from tensile or flexure testing.
4. Applications of this simple estimation method are discussed. A common notion that ductile metals always have high m values must be discarded. Causes of m reduction need to be considered as material variation, and test accuracies can affect the outcomes. The method can add a quantitative tool based on the Weibull theory to engineering practice.

Funding: This research received no external funding.

Acknowledgments: The author is grateful to Robert Gordon and Stephen Walley for providing historical strength documents, to Bruce Dunn for a statistics document and to K. Naito, G.F. Guo and L. Huang for supplying unpublished strength data.

Conflicts of Interest: The author declares no conflict of interest.

References

1. Weibull, W. A statistical theory of the strength of material. *Ing. Vetenskapa Acad. Handlingar* **1939**, *151*, 1–45.
2. Weibull, W. A statistical distribution function of wide applicability. *Trans. ASME J. Appl. Mech.* **1951**, *73*, 293–297.
3. Lai, C.-D.; Pra Murthy, D.N.; Xie, M. Weibull Distributions and Their Applications. In *Springer Handbook of Engineering Statistics*; Pham, H., Ed.; Springer: Cham, Switzerland, 2006; pp. 63–78.
4. Abernethy, R.B.; Breneman, J.E.; Medlin, C.H.; Reinman, G.L. *Weibull Analysis Handbook*; AFWAL-TR-83-2079; Pratt and Whitney Aircraft: North Palm Beach, FL, USA, 1983; 243p.
5. Abernethy, R.B. *The New Weibull Handbook*, 2nd ed.; Gulf Pub. Co.: North Palm Beach, FL, USA, 1996; 350p.
6. Song, K.W.; Chang, I.H.; Pham, H. A software reliability model with a Weibull fault detection rate function subject to operating environments. *Appl. Sci.* **2017**, *7*, 983. [[CrossRef](#)]
7. Rafsanjani, H.M.; Sørensen, J.D. Reliability analysis of fatigue failure of cast components for wind turbines. *Energies* **2015**, *8*, 2908–2923. [[CrossRef](#)]
8. Wang, C.; Wu, J.; Zhao, W. Reliability analysis and overload capability assessment of oil-immersed power transformers. *Energies* **2016**, *9*, 43. [[CrossRef](#)]
9. Fang, X.; Zhu, J.; Lin, Z. Effects of electrode composition and thickness on the mechanical performance of a solid oxide fuel cell. *Energies* **2018**, *11*, 1735. [[CrossRef](#)]
10. Ye, X.W.; Su, Y.H.; Xi, P.S. Statistical analysis of stress signals from bridge monitoring by FBG system. *Sensors* **2018**, *18*, 491. [[CrossRef](#)]
11. Robinson, E.Y. *Estimating Weibull Parameters for Materials*; JPL Tech. Memo. 33-580; Jet Propulsion Lab: Pasadena, CA, USA, 1972; 62p.
12. Batdorf, S.B. Some approximate treatments of fracture statistics for polyaxial tension. *Int. J. Fract.* **1977**, *13*, 5–11. [[CrossRef](#)]
13. Forquin, P.; Hild, F. A probabilistic damage model of the dynamic fragmentation process in brittle materials. *Adv. Appl. Mech.* **2010**, *44*, 1–72.
14. Trustrum, K.; Jayatilaka, A.d.S. On estimating the Weibull modulus for a brittle material. *J. Mater. Sci.* **1979**, *14*, 1080–1084. [[CrossRef](#)]
15. Ono, K. Size effects of high strength steel wires. *Metals* **2019**, *9*, 240. [[CrossRef](#)]
16. Ritter, J.E.; Bandyopadhyay, N.; Jakus, K. Statistical reproducibility of dynamic and static fatigue experiments. *Ceram. Bull.* **1981**, *60*, 798–806.
17. Canadian Standards Association (CSA). *Specification for Fibre Reinforced Polymers*; CSA S807-10; Canadian Standards Association: Rexdale, ON, Canada, 2017.
18. *ASTM D7957/D7957M-17. Standard Specification for Solid Round Glass Fiber Reinforced Polymer Bars for Concrete Reinforcement*; ASTM International: West Conshohocken, PA, USA, 2017; 5p.
19. American Concrete Institute (ACI) 440.6-08(17). *Specification for Carbon and Glass Fiber-Reinforced Polymer Bar Materials for Concrete Reinforcement*; American Concrete Institute: Farmington Hills, MI, USA, 2017.
20. Ross, R. Bias and standard deviation due to Weibull parameter estimation for small data sets. *IEEE Trans. Dielectr. Electr. Insul.* **1996**, *3*, 28–42. [[CrossRef](#)]
21. Yang, Y.; Li, W.; Tang, W.; Li, B.; Zhang, D. Sample sizes based on Weibull distribution and normal distribution for FRP tensile coupon test. *Materials* **2019**, *12*, 126. [[CrossRef](#)]
22. Alford, N.M.; Birchall, J.D.; Kendall, K. Engineering ceramics—The process problem. *Mater. Sci. Technol.* **1986**, *2*, 329–336. [[CrossRef](#)]
23. Mayrbaur, R.M.; Camo, S. *Guidelines for Inspection and Strength Evaluation of Suspension Bridge Parallel Wire Cables, Report 534*; National Cooperative Highway Research Program: Washington, DC, USA, 2004; 274p.
24. Haggag, F.M. *Round Robin Results of Interlaboratory Automated Ball Indentation (ABI) Tests by Task Group E 28.06.14*; ASTM International: West Conshohocken, PA, USA, 2003; 78p.
25. Ingelbrecht, C.; Loveday, M.S. *The Certification of Ambient Temperature Tensile Properties of a Reference Material for Tensile Testing According to EN 10002-1. CRM 661, EU Report 19589 EN*; European Commission: Geel, Belgium, 2000; 26p.
26. *ASTM C1499-15, Standard Test Method for Monotonic Equibiaxial Flexural Strength of Advanced Ceramics at ambient Temperature*; ASTM International: West Conshohocken, PA, USA, 2015; 13p.

27. Wetherhold, R.C. Statistical distribution of strength of fiber-reinforced composite materials. *Polym. Compos.* **1986**, *7*, 116–123. [[CrossRef](#)]
28. Van der Zwaag, S. The concept of filament strength and Weibull modulus. *J. Test. Eval.* **1989**, *17*, 292–298. [[CrossRef](#)]
29. Bazant, Z.P.; Planas, J. *Fracture and Size Effect in Concrete and Other Quasibrittle Materials*; CRC Press: Boca Raton, FL, USA, 1998; 616p.
30. Gong, J.; Li, Y. Relationship between the estimated Weibull modulus and the coefficient of variation of the measured fracture strength for ceramics. *J. Am. Ceram. Soc.* **1999**, *82*, 449–452. [[CrossRef](#)]
31. Deng, B.; Jiang, D. Determination of the Weibull parameters from the mean value and the coefficient of variation of the measured strength for brittle ceramics. *J. Adv. Ceram.* **2017**, *6*, 149–156. [[CrossRef](#)]
32. Wallin, K. *Master Curve Analysis of Ductile to Brittle Transition Region Fracture Toughness Round Robin Data: The “EURO” Fracture Toughness Curve*; VTT Publications 367; Technical Research Centre of Finland: Espoo, Finland, 1998; 58p.
33. *ASTM E1921-19, Standard Test Method for Determination of Reference Temperature, T_0 , for Ferritic Steels in the Transition Range*; ASTM International: West Conshohocken, PA, USA, 2019; 39p.
34. Mills, A.P. The old Essex-Merrimac Chain Suspension Bridge at Newburyport, Massachusetts, and tests of its wrought iron links after 100 years' service. *Eng. News* **1911**, *66*, 129–132.
35. Gordon, R.B. Strength and structure of wrought iron. *Archeomaterial* **1988**, *2*, 109–137.
36. Gordon, R.; Knopf, R. Evaluation of wrought iron for continued service in historic bridges. *J. Mater. Civ. Eng.* **2005**, *17*, 393–399. [[CrossRef](#)]
37. Kirkaldy, D. *Results of an Experimental Inquiry into the Comparative Tensile Strength and Other Properties of Various Kinds of Wrought Iron and Steel*; Bell & Bain: Glasgow, UK, 1863; 244p.
38. Bowman, M.D.; Piskorowski, A.M. *Evaluation and Repair of Wrought Iron and Steel Structures in Indiana*; FHWA/IN/JTRP-2004/4; Purdue Univ.: West Lafayette, IN, USA, June 2004; 240p.
39. Beardslee, L.A. *Experiments on the Strength of Wrought Iron and of Chain Cables, Report comm. Us Board to Test Iron, Steel and Other Metals, on Chain Cables, Malleable Iron, and Wrought Iron*; Government Printing Office: Washington, DC, USA, 1879; 138p.
40. Unwin, W.C. *The Testing of Materials of Construction*; Longmans, Green Co.: London, UK, 1910; pp. 334–342.
41. Percy, J. On steel wire of high strength. *J. Iron Steel Inst.* **1886**, *29*, 62–80.
42. Perry, R.J. Estimating strength of the Williamsburg Bridge suspension cables. *Am. Stat.* **1998**, *52*, 211–217.
43. Mahmoud, K.M. *BTC Method for Evaluation of Remaining Strength and Service Life of Bridges*; NYSDOT Report C-07-11; Bridge Technology Consulting: New York, NY, USA, 2011; pp. 21–24.
44. Ono, K. Structural materials: Metallurgy of bridges. In *Metallurgical Design and Industry, Prehistory to the Space Age*; Kaufman, B., Briant, C.L., Eds.; Springer: Cham, Switzerland, 2018; pp. 193–269.
45. Ganesan, P.; Boswell, R.H.; Smith, G.D.; Crum, J.R. Characterization of current production AOD+ESR Alloy 625 plate. In *Proceedings of the 4th International Symposium on Superalloys 718, 625, 706 and Derivatives, Pittsburgh, PA, USA, 15–18 June 1997*; Loria, E.A., Ed.; Minerals, Metals and Materials Society: Pittsburgh, PA, USA, 1997; pp. 763–797.
46. Chen, J.H.; Cao, R. Micromechanism of cleavage fracture of metals. In *A Comprehensive Microphysical Model for Cleavage Cracking in Metals*; Elsevier: Amsterdam, The Netherlands, 2015; pp. 141–443.
47. Salem, J.A. *Generalized Reliability Methodology Applied to Brittle Anisotropic Single Crystals*; NASA Report, NASA TM—2002-210519; Glenn Res. Center: Cleveland, OH, USA, 2002; 195p.
48. Simon, N.J.; Drexler, E.S.; Reed, R.P. *Properties of Copper and Copper Alloys at Cryogenic Temperatures*; NIST Monograph 177; National Institute of Standards and Technology: Boulder, CO, USA, 1992; 872p.
49. Catangiu, A.; Ungureanu, D.N.; Despa, V. Data scattering in strength measurement of steels and glass/epoxy composite. *Mater. Mech.* **2017**, *15*, 6. [[CrossRef](#)]
50. Fiał, C.; Ciał, A.; Czarski, A.; Sułowski, M. Fracture statistics using three-parameter and two-parameter Weibull distributions for Fe-0.4C-1.5Cr-1.5Ni-0.8Mn-0.2Mo structural sintered steel. *Arch. Metall. Mater.* **2016**, *61*, 1547–1554. [[CrossRef](#)]
51. Cacace, S.; Semeraro, Q. About fluence and process parameters on maraging steel processed by selective laser melting: Do they convey the same information? *Int. J. Precision Eng. Manuf.* **2018**, *19*, 1873–1884. [[CrossRef](#)]
52. Guo, S.; Liu, R.; Jiang, X.; Zhang, H.; Zhang, D.; Wang, J.; Pan, F. Statistical analysis on the mechanical properties of magnesium alloys. *Materials* **2017**, *10*, 1271. [[CrossRef](#)]

53. Lee, S.G.; Patel, G.R.; Gokhale, A.M.; Sreeranganathan, A.; Horstemeyer, M.F. Quantitative fractographic analysis of variability in the tensile ductility of high-pressure die-cast AE44 Mg-alloy. *Mater. Sci. Eng.* **2006**, *A427*, 255–262. [[CrossRef](#)]
54. Szymaszal, J.; Piątkowski, J.; Przoncziono, J. Determination of reliability index and Weibull modulus as a measure of hypereutectic silumins survival. *Arch. Foundry Eng.* **2007**, *7*, 237–240.
55. Lu, C. A reassessment of the strength distributions of advanced ceramics. *J. Aust. Ceram. Soc.* **2008**, *44*, 38–41.
56. Tinschert, J.; Zwez, D.; Marx, R.; Anusavice, K.J. Structural reliability of alumina-, feldspar-, leucite-, mica- and zirconia-based ceramics. *J. Dent.* **2000**, *28*, 529–535. [[CrossRef](#)]
57. Ćurković, L.; Bakić, A.; Kodvanj, J.; Haramina, T. Flexural strength of alumina ceramics: Weibull analysis. *Trans. Famena* **2010**, *34*, 13–19.
58. Scapin, M.; Peroni, L.; Avalle, M. Dynamic Brazilian test for mechanical characterization of ceramic ballistic protection. *Shock Vib.* **2017**, *2017*, 7485856. [[CrossRef](#)]
59. Klein, C.A. Flexural strength of sapphire: Weibull statistical analysis of stressed area, surface coating, and polishing procedure effects. *J. Appl. Phys.* **2004**, *96*, 3172–3179. [[CrossRef](#)]
60. Basu, B.; Tiwari, D.; Kundu, D.; Prasad, R. Is Weibull distribution the most appropriate statistical strength distribution for brittle materials? *Ceram. Int.* **2009**, *35*, 237–246. [[CrossRef](#)]
61. Duffy, S.F.; Powers, L.M.; Starlinger, A. Reliability analysis of structural ceramic components using a three-parameter Weibull distribution. In *Proceedings of the 37th International Gas Turbine and Aeroengine Congress and Exposition, Cologne, Germany, 1–4 June 1992*; American Society of Mechanical Engineers: New York, NY, USA; 12p.
62. Klein, C.A. Characteristic strength, Weibull modulus, and failure probability of fused silica glass. *Opt. Eng.* **2009**, *48*, 113401. [[CrossRef](#)]
63. Quinn, J.; Quinn, G.D. A practical and systematic review of Weibull statistics for reporting strengths of dental materials. *Dent. Mater.* **2010**, *26*, 135–147. [[CrossRef](#)] [[PubMed](#)]
64. Nakamura, Y.; Hojo, S.; Sato, H. The effect of surface roughness on the Weibull distribution of porcelain strength. *Dent. Mater. J.* **2010**, *29*, 30–34. [[CrossRef](#)]
65. Roos, M.; Schatz, C.; Stawarczyk, B. Two independent prospectively planned blinded Weibull statistical analyses of flexural strength data of zirconia materials. *Materials* **2016**, *9*, 512. [[CrossRef](#)]
66. Li, H.; Gao, M.; Sun, L. *Strength Weibull distribution analysis for the NBG-18 graphite in HTR Trans, SMiRT 19, Toronto, ON, Canada, 12–17 August 2007*; Paper # S03/4; International Association for Structural Mechanics in Reactor Technology: Raleigh, NC, USA, 2007; 4p.
67. Bona, A.D.; Anusavice, K.J.; DeHoff, P.H. Weibull analysis and flexural strength of hot-pressed core and veneered ceramic structures. *Dent. Mater.* **2003**, *19*, 662–669. [[CrossRef](#)]
68. Cordell, J.M.; Vogl, M.L.; Johnson, A.J.W. The influence of micropore size on the mechanical properties of bulk hydroxyapatite and hydroxyapatite scaffolds. *J. Mech. Behav. Biomed.* **2009**, *2*, 560–570. [[CrossRef](#)] [[PubMed](#)]
69. Fan, X.; Casea, E.D.; Rena, F.; Shua, Y.; Baumann, M.J. Part I: Porosity dependence of the Weibull modulus for hydroxyapatite and other brittle materials. *J. Mech. Behav. Biomed.* **2012**, *8*, 21–36. [[CrossRef](#)] [[PubMed](#)]
70. Wilson, D.M. Statistical tensile strength of Nextel 610 and Nextel 720 fibers. *J. Mater. Sci.* **1997**, *32*, 2535–2542. [[CrossRef](#)]
71. Pai, D.; Yarmolenko, S.; Freeman, E.; Sankar, J.; Zawada, L.P. Effect of monazite coating on tensile behavior of Nextel 720 fibers at high temperatures. In *Proceedings of the 28th International Conference on Advanced Ceramics and Composites B: Ceramic Engineering and Science*; Lara-Curzio, E., Readey, M.J., Eds.; American Ceramic Society: Westerville, OH, USA, 2008; pp. 117–122.
72. Kotchick, D.M.; Hink, R.C.; Tressler, R.E. Gauge length and surface damage effects on the strength distributions of silicon carbide and sapphire filaments. *J. Compos. Mater.* **1975**, *9*, 327–336. [[CrossRef](#)]
73. Scott, W.D.; Gaddipatti, A. *Strength of Long Glass Fibers*; Final Report, 1 Sep. 1977; Univ. Wash.: Seattle, WA, USA, 1977; 34p.
74. Holt, N.L.; Finnie, I. *Fracture and Fatigue of High Strength Filaments*; Final Report 9/25/1974-8/30/1975; Univ Illinois: Urbana, IL, USA, 1975; 107p. [[CrossRef](#)]
75. Smith, W.L.; Michalske, T.A. *Inert Strength of Pristine Silica Glass Fibers*; SAND92-1107; Sandia National Lab: Albuquerque, NM, USA, 1993; 4p.

76. Zinck, P.; Pays, M.F.; Rezakhanlou, R.; Gerard, J.F. Mechanical characterisation of glass fibres as an indirect analysis of the effect of surface treatment. *J. Mater. Sci.* **1999**, *34*, 2121–2133. [[CrossRef](#)]
77. Lund, M.D.; Yue, Y. Fractography and tensile strength of glass wool fibres. *J. Ceram. Soc. Jpn.* **2008**, *116*, 841–845. [[CrossRef](#)]
78. Ma, L.; Sines, G. *Strength of Carbon Fibers with Various Gauge Lengths and the Optimum Weibull Moduli*; UCLA-MSE Report; Univ. Calif. Los Angeles: Los Angeles, CA, USA, 1995; pp. 56–57. Available online: https://acs.omnibooksonline.com/data/papers/1995_56.pdf (accessed on 24 February 2019).
79. Naito, K.; Tanaka, Y.; Yang, J.M.; Kagawa, Y. Tensile properties of ultrahigh strength PAN-based, ultrahigh modulus pitch-based and high ductility pitch-based carbon fibers. *Carbon* **2008**, *46*, 189–195. [[CrossRef](#)]
80. Naito, K.; Tanaka, Y.; Yang, J.M. Transverse compressive properties of polyacrylonitrile (PAN)-based and pitch-based single carbon fibers. *Carbon* **2017**, *118*, 168–183. [[CrossRef](#)]
81. Flores, O.; Bordia, R.K.; Bernard, S.; Uhlemann, T.; Krenkel, W.; Motz, G. Processing and characterization of large diameter ceramic SiCN monofilaments from commercial oligosilazanes. *RSC Adv.* **2015**, *5*, 107001. [[CrossRef](#)]
82. Neilson, H. Weibull Modulus of Hardness, Bend Strength, and Tensile Strength of Ni-Ta-Co-X Metallic Glass Ribbons. Master's Thesis, Case Western Reserve University, Pittsburgh, PA, USA, 2014; 120p.
83. Bansal, N.P. *Effects of HF Treatments on Tensile Strength of Hi-Nicalon Fibers*; NASA/TM-1998-206626; Lewis Res Center: Cleveland, OH, USA, 1998; 22p.
84. Rohen, L.A.; Margem, F.M.; Neves, A.C.C.; Gomes, M.A.; Monteiro, S.N.; Vieira, C.M.F.; de Castro, R.G.; Borges, G.X. Weibull Analysis of the behavior on tensile strength of hemp fibers for different intervals of fiber diameters. In *Characterization of Minerals, Metals, and Materials 2015*; Carpenter, J.S., Bai, C., Pablo Escobedo-Diaz, J., Hwang, J.-Y., Ikhmayies, S., Li, B., Li, J., Neves, S., Peng, Z., Zhang, M., Eds.; Springer: Cham, Switzerland, 2015; pp. 123–130.
85. Wang, F.; Shao, J. Modified Weibull distribution for analyzing the tensile strength of bamboo fibers. *Polymers* **2014**, *6*, 3005–3018. [[CrossRef](#)]
86. Tagawa, T.; Miyata, T. Size effect on tensile strength of carbon fibers. *Mater. Sci. Eng. A* **1997**, *A238*, 336–342. [[CrossRef](#)]
87. Tanaka, T.; Nakayama, H.; Sakaida, A.; Horikawa, N. Estimation of tensile strength distribution for carbon fiber with diameter varying along fiber. *J. Soc. Mater. Sci. Jpn.* **1998**, *47*, 719–726. [[CrossRef](#)]
88. Naito, K.; Yang, J.M.; Inoue, Y.; Fukuda, H. The effect of surface modification with carbon nanotubes upon the tensile strength and Weibull modulus of carbon fibers. *J. Mater. Sci.* **2012**, *47*, 8044–8051. [[CrossRef](#)]
89. Naito, K. Stress analysis and fracture toughness of notched polyacrylonitrile (PAN)-based and pitch-based single carbon fibers. *Carbon* **2018**, *126*, 346–359. [[CrossRef](#)]
90. Koyanagi, J.; Hatta, H.; Kotani, M.; Kawada, K. A comprehensive model for determining tensile strengths of various unidirectional composites. *J. Compos. Mater.* **2009**, *43*, 1901–1914. [[CrossRef](#)]
91. Naresh, K.; Shankar, K.; Velmurugan, R. Reliability analysis of tensile strengths using Weibull distribution in glass/epoxy and carbon/epoxy composites. *Compos. Part B* **2018**, *133*, 129–144. [[CrossRef](#)]
92. Jin, S.J. Reliability-Based Characterization of Prefabricated FRP Composites for Rehabilitation of Concrete Structures. Master's Thesis, University California San Diego, La Jolla, CA, USA, 2008; 235p.
93. Naito, K.; Yang, J.M.; Kagawa, Y. Tensile properties of high strength polyacrylonitrile (PAN)-based and high modulus pitch-based hybrid carbon fibers-reinforced epoxy matrix composite. *J. Mater. Sci.* **2012**, *47*, 2743–2751. [[CrossRef](#)]
94. Naito, K.; Oguma, H. Tensile properties of novel carbon/glass hybrid thermoplastic composite rods. *Compos. Struct.* **2017**, *161*, 23–31. [[CrossRef](#)]
95. Okeil, A.M. *Characterization of Mechanical Properties of Composite Materials for Infrastructure Projects*; Final Report, Project #13-02; Louisiana State University: Baton Rouge, LA, USA, June 2013; 39p.
96. Vardhan, A.V.; Charan, V.S.S.; Raj, S.; Hussaini, S.M.; Rao, G.V. Failure prediction of CFRP composites using Weibull analysis. *AIP Conf. Proc.* **2019**, *2057*, 020014. [[CrossRef](#)]
97. Ma, Y.; Yang, Y.; Sugahara, T.; Hamada, H. A study on the failure behavior and mechanical properties of unidirectional fiber reinforced thermosetting and thermoplastic composites. *Compos. Part B Eng.* **2016**, *99*, 162–172. [[CrossRef](#)]
98. Dirikolu, M.H.; Aktaş, A.; Birgoren, B. Statistical analysis of fracture strength of composite materials using Weibull distribution. *Turk. J. Eng. Environ. Sci.* **2002**, *26*, 45–48.

99. Zhao, D.; Hamada, H.; Yang, Y. Influence of polyurethane dispersion as surface treatment on mechanical, thermal and dynamic mechanical properties of laminated woven carbon fiber-reinforced polyamide 6 composites. *Compos. Part B Eng.* **2018**, *160*, 535–545. [[CrossRef](#)]
100. Ou, Y.; Zhu, D.; Zhang, H.; Huang, L.; Yao, Y.; Li, G.; Mobasher, B. Mechanical characterization of the tensile properties of glass fiber and its reinforced polymer (GFRP) composite under varying strain rates and temperatures. *Polymers* **2016**, *8*, 196. [[CrossRef](#)] [[PubMed](#)]
101. Arczewska, P.; Polak, M.A.; Penlidi, A. Relation between tensile strength and modulus of rupture for GFRP reinforcing bars. *J. Mater. Civ. Eng.* **2019**, *31*, 04018362. [[CrossRef](#)]
102. Ramakrishnan, M.U. Strength and failure characteristics of SMC-R composites under biaxial loads. Master's Thesis, Univ. Michigan, Dearborn, MI, USA, 2017; p. 46.
103. Rodrigues, S.A., Jr.; Ferracane, J.L.; Bona, A.D. Flexural strength and Weibull analysis of a microhybrid and a nanofill composite evaluated by 3- and 4-point bending tests. *Dent. Mater.* **2008**, *24*, 426–431.
104. Miranda, R.B.d.P.; Miranda, W.G., Jr.; Ricci, D.R.; Ussui, V.L.; Marchi, J.; Cesar, P.F. Effect of titania content and biomimetic coating on the mechanical properties of the Y-TZP/TiO₂ composite. *Dent. Mater.* **2018**, *34*, 238–245. [[CrossRef](#)]
105. Yang, W.; Araki, H.; Kohyama, A.; Busabok, C.; Hu, Q.; Suzuki, H.; Noda, T. Flexural strength of a plain-woven Tyranno-SA fiber-reinforced SiC matrix composite. *Mater. Trans.* **2003**, *44*, 1797–1801. [[CrossRef](#)]
106. Pétursson, J. Performance characterization of ceramic matrix composites through uniaxial monotonic tensile testing. Master's Thesis, Embry-Riddle Aeronautical University, Daytona Beach, FL, USA, December 2016; p. 31.
107. ASTM E8/E8M-16a, *Standard Test Methods for Tension Testing of Metallic Materials*; ASTM International: West Conshohocken, PA, USA, 2016; 30p.
108. Loveday, M.S.; Gray, T.; Aegerter, J. *Tensile Testing of Metallic Materials: A Review*; Tenstand—Work Package 1—Final Report, April 2004; National Physical Lab: Teddington, UK, 2005; 171p.
109. Qin, J.; Chen, R.; Wen, K.; Lin, Y.; Liang, M.; Lu, F. Mechanical behaviour of dual-phase high-strength steel under high strain rate tensile loading. *Mater. Sci. Eng.* **2013**, *A586*, 62–70. [[CrossRef](#)]
110. Krawczyńska, A.T.; Gloc, M.; Lublinska, K. Intergranular corrosion resistance of nanostructured austenitic stainless steel. *J. Mater. Sci.* **2013**, *48*, 4517–4523. [[CrossRef](#)]
111. Shi, X.; Zeng, W.; Sun, Y.; Guo, P. Microstructure-tensile properties correlation for the Ti-6Al-4V titanium alloy. *J. Mater. Eng. Perform.* **2015**, *24*, 1754–1762. [[CrossRef](#)]
112. Staller, O.; Mitterbauer, C.; Mayr, K. Tensile strengths and Young's modulus of thin copper and copper-nickel (CuNi44) substrates. *Cent. Eur. J. Chem.* **2006**, *6*, 535–541. [[CrossRef](#)]
113. Podgornik, B.; Žužek, B.; Sedlaček, M.; Kevorkijan, V.; Hostej, B. Analysis of factors influencing measurement accuracy of Al alloy tensile test results. *Meas. Sci. Rev.* **2016**, *16*, 1–7. [[CrossRef](#)]
114. Brindha, M.; Kurunji Kumaran, N.; Rajasigamani, K. Evaluation of tensile strength and surface topography of orthodontic wires after infection control procedures: An in vitro study. *Dent. Sci.* **2014**, *6*, 44–48. [[CrossRef](#)]
115. Sato, K. Improving the Toughness of Ultrahigh Strength Steel. Ph.D. Thesis, University Calif. Berkeley, Berkeley, CA, USA, 2002; 166p.
116. Wallin, K.; Saario, T.; Törrönen, K. Theoretical scatter in brittle fracture toughness results described by the Weibull distribution. In *Application of Fracture Mechanics to Materials and Structures*; Sih, G.C., Sommer, E., Dahl, W., Eds.; Springer: Dordrecht, The Netherlands, 1984. [[CrossRef](#)]
117. Mäder, E.; Liu, J.; Hiller, J.; Lu, W.; Li, Q.; Zhandarov, S.; Chou, T.-W. Coating of carbon nanotube fibers: Variation of tensile properties, failure behavior, and adhesion strength. *Front. Mater.* **2015**, *2*, 53. [[CrossRef](#)]
118. Barber, A.H.; Andrews, R.; Schadler, L.S.; Wagner, H.D. On the tensile strength distribution of multiwalled carbon nanotubes. *Appl. Phys. Lett.* **2005**, *87*, 203106. [[CrossRef](#)]
119. Sun, G.; Pang, J.H.L.; Zhou, J.; Zhang, Y.; Zhan, Z.; Zheng, L. A modified Weibull model for tensile strength distribution of carbon nanotube fibers with strain rate and size effects. *Appl. Phys. Lett.* **2012**, *101*, 131905. [[CrossRef](#)]
120. Pugno, N.M.; Ruoff, R.S. Nanoscale Weibull statistics. *J. Appl. Phys.* **2006**, *99*, 024301. [[CrossRef](#)]
121. Xu, X.F.; Beyerlein, I.J. Probabilistic strength theory of carbon nanotubes and fibers, Chap. 5. In *Advanced Computational Nanomechanics*; Silvestre, N., Ed.; Wiley: Chichester, UK, 2016; pp. 123–146.
122. Mayrbaur, R.M. Wire test results for three suspension bridge cables. In *Advances in Cable-Supported Bridges*; Mahmoud, K.M., Ed.; Taylor & Francis: London, UK, 2006; pp. 127–144.

123. Kittl, P.; Diaz, G.; Morales, M. Determination of Weibull's parameters on flexure strength of round beams of aluminum-copper alloy and cast iron. *Theor. Appl. Fract. Mech.* **1990**, *13*, 251–255. [[CrossRef](#)]
124. Holland, F.A., Jr.; Zaretsky, E.V. Investigation of Weibull statistics in fracture analysis of cast aluminum. *Trans. ASME* **1990**, *112*, 246–254. [[CrossRef](#)]
125. Green, N.R.; Campbell, J. Statistical distributions of fracture strengths of cast Al-7Si-Mg alloy. *Mater. Sci. Eng.* **1993**, *A173*, 261–266. [[CrossRef](#)]
126. Eisaabadi B, G.; Davami, P.; Kim, S.K.; Tiryakioğlu, M. The effect of melt quality and filtering on the Weibull distributions of tensile properties in Al-7%Si-Mg alloy castings. *Mater. Sci. Eng.* **2013**, *A579*, 64–70. [[CrossRef](#)]
127. Shevidi, A.H.; Taghiabadi, R.; Razaghian, A. Weibull analysis of effect of T6 heat treatment on fracture strength of AM60B magnesium alloy. *Trans. Nonferrous Met. Soc. China* **2018**, *28*, 20–29. [[CrossRef](#)]
128. ASTM C1239-13, *Standard Practice for Reporting Uniaxial Strength Data and Estimating Weibull Distribution Parameters for Advanced Ceramics*; ASTM International: West Conshohocken, PA, USA, 2018; 18p.
129. Bright, G.W.; Kennedy, J.I.; Robinson, F.; Evans, M.; Whittaker, M.T.; Sullivan, J.; Gao, Y. Variability in the mechanical properties and processing. *Procedia Eng.* **2011**, *10*, 106–111. [[CrossRef](#)]
130. Hess, P.E.; Bruchman, D.; Assakkaf, I.A.; Ayyub, B.M. Uncertainties in material and geometric strength and load variables. *Naval Eng. J.* **2008**, *114*, 139–166. [[CrossRef](#)]
131. Hou, J.; Fu, S.; An, X.; He, Y. Study on statistical characteristic of strength of steel plate used for penstocks of hydropower stations. In Proceedings of the 15th World Congress on Non-Destructive Testing, Rome, Italy, 15–21 October 2000; p. 444.
132. Sadowski, A.J.; Rotter, J.M.; Reinke, T.; Ummenhofer, T. Statistical analysis of the material properties of selected structural carbon steels. *Struct. Saf.* **2014**, *53C*, 26–35. [[CrossRef](#)]
133. Da Silva, L.S.; Rebelo, C.; Nethercot, D.; Marques, L.; Simões, R.; Vila Real, P.M.M. Statistical evaluation of the lateral-torsional buckling resistance of steel I-beams, Part 2: Variability of steel properties. *J. Construct. Steel Res.* **2009**, *65*, 832–849. [[CrossRef](#)]
134. Schmidt, B.J.; Bartlett, F.M. Review of resistance factor for steel: Data collection. *Can. J. Civil Eng.* **2002**, *29*, 98–102. [[CrossRef](#)]
135. Andriono, T.; Park, R. Seismic design considerations of the properties of New Zealand manufactured steel reinforcing bars. *Bull. N. Z. Natl. Soc. Earthq. Eng.* **1986**, *19*, 213–246.
136. Djavanroodi, F.; Salman, A. Variability of mechanical properties and weight for reinforcing bar produced in Saudi Arabia. *IOP Conf. Ser. Mater. Sci. Eng.* **2017**, *230*, 012002. [[CrossRef](#)]
137. Belmonte, H.M.S.; Mulheron, M.; Smith, P.A.; Ham, A.; Wescombe, K.; Whiter, J. Weibull-based methodology for condition assessment of cast iron water mains and its application. *Fatigue Fract. Eng. Mater. Struct.* **2008**, *31*, 370–385. [[CrossRef](#)]
138. Shah, S.; Panda, S.K.; Khan, D. Weibull analysis of H-451 nuclear-grade graphite. *Procedia Eng.* **2016**, *144*, 366–373. [[CrossRef](#)]
139. Rainer, A.; Capell, T.F.; Clay-Michael, N.; Demetriou, M.; Evans, T.S.; Jesson, D.A.; Mulheron, M.J.; Scudder, L.; Smith, P.A. What does NDE need to achieve for cast iron pipe networks? *Infrastruct. Asset Manag.* **2017**, *42*, 68–82. [[CrossRef](#)]
140. Ono, K. Review on structural health evaluation with acoustic emission. *Appl. Sci.* **2018**, *8*, 958. [[CrossRef](#)]

